Università degli Studi di Torino
Doctoral School of the University of Torino
PhD Programme in Chemical and Materials Sciences XXXIV Cycle

Use of polarized light for the assessment of new generation display

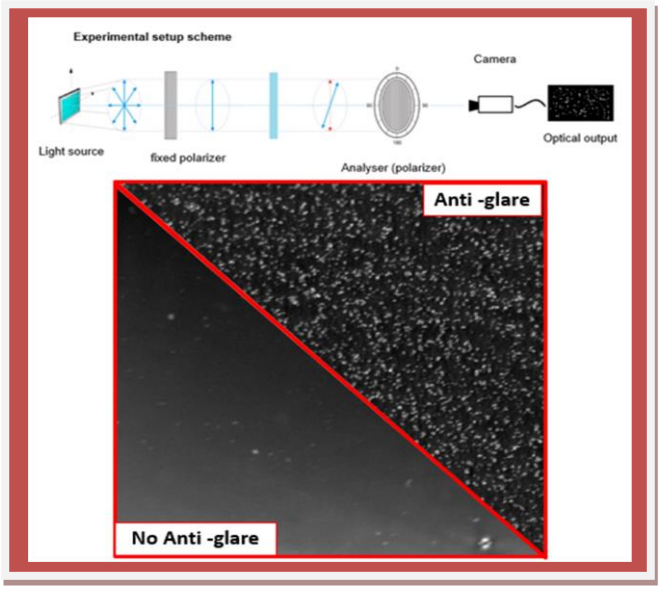

Fabio Scaffidi Muta

Supervisor:
Prof. Ettore Vittone
Co-supervisor:
Dr. Nello Li Pira

Università degli Studi di Torino

Doctoral School of the University of Torino

PhD Programme in Chemical and Materials Sciences XXXIV cycle

Use of polarized light for the assessment of new generation display

Candidate: **Fabio Scaffidi Muta**

Supervisor: Prof. **Ettore Vittone**

Jury Members:

Dr. **Boeffel Christine**
Fraunhofer Institute for Applied Polymer Research
Functional Materials and Devices

Prof. **Rafailov Edik**
School of Engineering and Applied Science, Aston University
Aston Institute of Photonics Technology

Prof. **Truccato Marco**
University of Turin
Physics Department

Head of the Doctoral School: Prof. Alberto Rizzuti

PhD Programme Coordinator: Prof. Bartolome Civalleri

Torino, 2022

Outline

List of abbreviations

ACF: Auto-Correlation Function
AF: Anti-Fingerprint
AG: Anti-Glare
AM: Anti-microbial
AMOLED: Active-Matrix Organic Light Emitting Diode
AR: Anti-Reflective
CCD: Charge Coupled Device
CIE: International Commission on Illumination

CRF: Centro Ricerche FIAT
FCA: FIAT Chrysler Automobile
FTIR: Fourier Transform Infrared spectroscopy
EDS: Energy Dispersive X-Ray Spectrometry
GU: Gloss Unit
HC: Hard Coat
HDR: High Dynamic Range
IML: In Mold Labelling
ISO: International Organization for Standardization
ITO: Indium Thin Oxide
LCD: Liquid Crystal Display
LED: Light Emitting Diode
OCA: Optical clear Adhesive
OCR: Optical Clear Resin
OLED: Organic Light Emitting Diode
PC: Polycarbonate
PET: Poly (ethylene terephthalate)
PMMA: Poly (methyl methacrylate)
PMOLED: Passive Matrix OLED
PP: Polypropylene
PPD: pixel Power Deviation
PVD: Physical Vapour Deposition
R2R: Roll to Roll
TFT: Thin Film Transistor
UV: Ultra-Violet

1. Introduction

The activities described in this work were performed in collaboration with **Centro Ricerche FIAT (CRF),** in the division **Materials & Sustainability Engineering**. In particular, the laboratory activities were done in the **Optics & Glazing Materials** group. This work addresses some of the main future challenges in automotive materials for **display coverlens**.

1.1. Scope of the thesis

Global automotive display market is flourishing driven by technological innovations such as car connectivity and development of infotainment systems. Automotive displays are the type of prime display or indicators of the status and any features employed on the vehicle. It also consists of the infotainment features on the display pane as it focuses on increasing the aesthetic appeal of the interiors of the vehicles. The trend is to increase the area of display with consequent increase of the geometry complexity of the display screen: seamless, flexible and conformable display will be a core feature in cars of the future.

The application of new device solutions for automotive display requires a deep investigation in terms of reliability, robustness and optical properties of the solutions. The assessment of reliability and robustness of the components is required to guarantee a lifetime of them equal to that of the vehicles. Instead, the assessment of the optical properties has the important role to give the components the desired aesthetical aspect and, at the same time, guarantee the readability of the display screen under different ambient conditions. The technologies and materials that enable the quality of the image are the coatings as well as the materials used in the coverlens, from bulk resins (or glasses) to optical adhesives. The activities described in this work are focused on the characterization of **materials for automotive display cover lens**. In particular, the scope of this thesis is to find a correlation between the materials involved in the production of automotive display cover lenses and the morphological and optical properties of the devices.

1.2. Objectives

The principal and main objectives of my work are:

1. the investigation of materials used in the commercial products for automotive display cover lenses. In particular, the activity is focused on the assessment of materials for **anti-glare coatings** (AG)
2. the assessment of morphological properties of anti-glare commercial products
3. the assessment of optical properties of anti-glare commercial products
4. the development of a new experimental method for the detection and quantification of **sparkle effect**, a transmission artefact where the displayed image appears to be covered by small, coloured highlights that scintillate with movement of the display and observer. In particular, the main objective is to quantify the sparkle effect due to the interaction of the light emitted by the display and the **anti-glare coating** applied on top of the coverlens.

2. Display in automotive: architectures and involved materials

This section describes the principal characteristics of an automotive display, which are the main mechanical structures, including materials used for the manufacturing of the different parts of the component itself. In the following paragraphs the deposition techniques of the functional coatings and the main techniques for the manufacturing of display cover lenses are reported and in depth described.

2.1. Introduction

Global automotive display market is flourishing driven by technological innovations such as car connectivity and development of infotainment systems. Automotive displays are the type of prime display or indicators of the status and any features employed on the vehicle. It also consists of the infotainment features on the display pane as it focuses on increasing the aesthetic appeal of the interiors of the vehicles. These displays are focused on acting as an information and entertainment liaison between the driver or passenger and the status of the vehicle in addition to the entertainment outlets [1]. The earlier idea of having a small screen for the central console for basic operations is completely changed with new, larger, more efficient and technically advanced displays. An example of small screen for the central console is illustrated in Figure 1.

Figure 1: FIAT Punto infotainment display (year 2010) [2]

The idea to have more efficient and technically advanced displays has been carried on from most of the car manufacturers. Figure 2 shows two models in production starting from 2020 from Mercedes – Benz S Class and FIAT 500 BEV (Battery Electrical Vehicle), in which not only the central information displays have different characteristics referred to the past, but also the traditional analogic instrument panels were changed with digital ones.

Figure 2: Mercedes-Benz S Class interiors (top image [3]) and FIAT 500BEV interiors (bottom image [4])

Infotainment & navigation systems have become standard features in most cars, whereas luxury car manufacturers have been shifting to the digital instrument clusters, multiple displays in car cabins, rear seat entertainment displays and head-up displays [5]. Car manufacturers are implementing integrated digital instrument clusters and digital central stacks that display more information and have more functionalities. The trend is to increase the area and the number of displays with consequent increase of the geometry complexity of the display screen.

Automotive display market is expected to grow at a compound annual growth rate of 9.5% in the forecast period of 2021 to 2028. The increasing need for in-vehicle entertainment is influencing the growth of automotive display market. Moreover, the increasing demand for digital instrument clusters is also flourishing the growth of the automotive display market [1]. The next section describes the structure of an automotive display, the materials and the manufacturing technologies involved.

2.2. Automotive display structure

An automotive display has a complex structure (see Figure 3): different materials are combined to promise high performances and functionalities; the mechanical and optical properties of these materials are important to give the better experiences to customers.

The automotive display is characterized by three main components: the **light source**, the **touch panel sensor,** and the **cover lens**. Different technologies can be used as light source: Liquid Crystal Display (LCD), AMOLED (Active-Matrix Organic Light Emitting Diode), PMOLED (Passive Matrix OLED), LED and others. Currently, most of the panels used in display systems are TFT (Thin Film Transistor) LCD, whereas OLED panels are expected to be adopted more prominently in automobiles soon. Due to the use of organic materials and thin plastic substrates, OLED panels provide design flexibility, including transparent displays [7]. In combination with LCD, a polarizer is applied on top of the screen to create a clearer, brighter image.

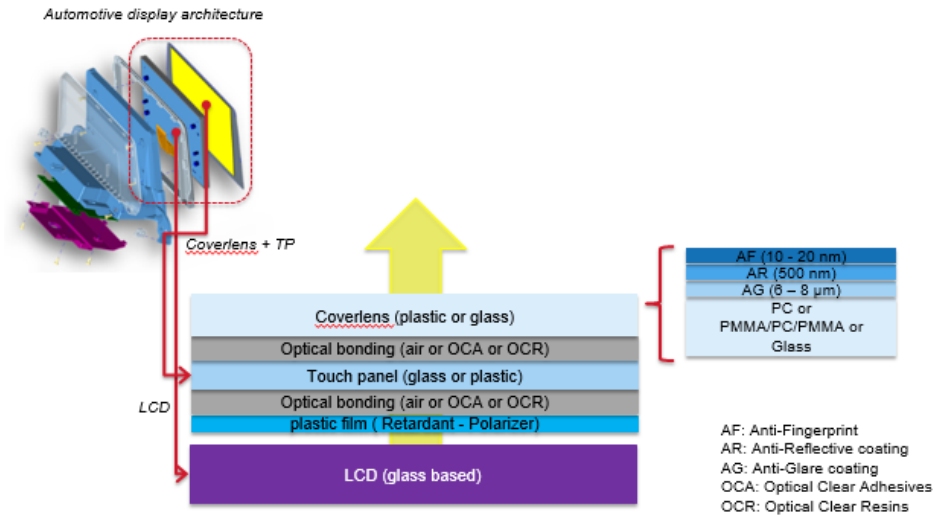

Figure 3: Example of automotive display architecture and coverlens structure

The second important component of an automotive display is the touch panel sensor. Different technology can be used: resistive touch panels and capacitive touch panels. The most widespread technology is the capacity touch sensor for the following purpose:

- It is suitable for large size monitors. It can be employed for applications that are large size (over 12 inch) with high resolution, high response speed and high durability
- Surface capacitive sensor can respond to light touch, and no pressure force is needed for detection
- Visibility is high because structure is only one glass layer (resistive touch sensors required two glass layers)
- It does not get affected by moist, dust, or grease
- Surface capacitive can detect touches by fingers only. Surface capacitive technology does not support multi-touch
- Surface capacitive touch screen is likely to be affected by noise. Recently, tolerance for noise has been improved with various methods such as noise shielding.

The touch sensor is in general characterized by a glass substrate with an ITO (Indium Thin Oxide) coating on the surface as electrode. The development of new touch

sensor for flexible and curved displays is requiring the application of flexible and formable touch sensors. These new solutions are based on plastic substrate, as PET (polyethylene terephthalate), with transparent electrodes (e.g., ITO), metal mesh (copper or silver based) and metal nano wires (e.g., silver).

The touch panel is physically bonded to the display with materials called optical bonding. The materials normally used are OCA (Optical clear Adhesive), OCR (Optical Clear Resin) or simply air. The OCAs are typically based on silicone materials, whilst OCRs are based on epoxy resins. The materials used for the optical bonding application must have properties which do not determine a change of the optical properties of the display. In particular, the materials must have high luminous transmittance, be colourless and the presence of visible defects (i.e., bubbles) must be avoided. The optical bonding is also used to bond the touch panel with the third important element of an automotive display: the cover lens.

The cover lens protects the display to mechanical stresses, functional touches and external potential damages. The display cover lenses are characterized from the following materials:

- Polycarbonate (PC)
- Poly (methyl methacrylate) (PMMA),
- Glass, in particular borosilicate

PC can be made from a variety of bifunctional alcohols, but most polymers are made with bisphenol A. Polycarbonates are a group of thermoplastic polymers containing carbonate groups in their chemical structures. PC has a wide application in automotive display thanks to its properties: extreme toughness, high heat distortion temperature, very good electrical insulation characteristics and excellent transparency. Its main disadvantages are the need to dry before processing, limited resistance to chemicals and UV light, and notch sensitivity [8]. Cover lenses based on PC material can be moulded and thermoformed. The injection moulding process used for PC enables breakthrough styling for innovative designs as well as cost-effective part integration.

PMMA, also known as acrylic glass or Plexiglas, is a transparent thermoplastic that is frequently used in sheet form as a lightweight or shatter-resistant alternative to glass. It is popular due to its moderate properties, ease of handling and processing

and low cost. Non-modified PMMA is brittle when subjected to load, particularly impact force. It is more prone to scratching than conventional inorganic glass, but modified PMMA can sometimes achieve high scratch and impact resistance. Due to its refractive index, PMMA has high light transmissivity (up to 92%) and it reflects about 4% of each surface (in the visible range). It filters ultraviolet (UV) light with wavelengths shorter than 300nm (like ordinary window glass). To improve absorption in the 300–400nm range, some manufacturers coat or add additives to PMMA. PMMA transmits infrared light with wavelengths up to 2800nm. Coloured PMMA varieties allow specific IR wavelengths to pass while blocking visible light [9]. When tensile strength, flexural strength, transparency, polish ability, and UV tolerance are more important than impact strength, chemical resistance, and heat resistance, PMMA is a cost-effective alternative to polycarbonate (PC) [10].

Glass is the name given to all amorphous bodies that are obtained by lowering the temperature of a melt independently of its chemical composition and the temperature range of solidification, which, because of the gradual increase of viscosity, adopts the mechanical properties of a solid body. Glass is melted at a temperature between 1000 and 2000°C. The structure of glass is not crystalline [11]. The main properties of glass are the high transparency, chemically inert, durable and glass shows tuneable (controlling the composition and the morphology) thermal expansion coefficient, which is a crucial thermal parameter in many applications. Regarding the mechanical properties, in general, glass is a brittle material, but the mechanical strength can be improved with thermal or chemical strengthening [12]. For display cover lenses application, typically, chemical strengthened glasses are used. Chemically strengthened glass is a material that has been treated with a chemical process after it was manufactured to give it stronger properties. The chemical process is called ion-exchange reaction. During this process, glass is submerged in a bath of potassium salt or potassium nitrate at 300 degrees Celsius. The bath is not hot enough to melt the glass, but the relatively high temperature allows the potassium nitrate to react with the surface of the glass, causing ions to be exchanged and compacted, thereby strengthening the glass. The glass sits in the bath for up to 30 hours in order to complete the chemical reaction, and then it is removed. The result is called chemically strengthened glass. Glass that has been chemically strengthened is usually about six to eight times the strength of float glass (thermal strengthening) [13].

Generally, the materials used for the display cover lenses have on top functional coatings to minimize sunlight reflection and to give reliable and suitable mechanical resistance. Examples of functional coatings are anti-reflective (AR), anti-fingerprint (AF), anti-glare (AG), hard coat (HC) or anti-microbial (AM). Typically, automotive display coverlens have on top one or a combination of these functional coatings.

The treatments can be performed with different processes:

- deposition of the coating directly on the substrate
- etching or texturing of the cover lens surface for anti-glare characteristics
- deposition of the coating on foils

The choice of the above-mentioned processes is determined from the selection of the cover lens manufacturing and the material selection of the cover lens substrate. Usually, the deposition directly on the substrate (physical vapour deposition process, see paragraph 2.4) is performed for the deposition of AR coating on glass. The etching or texturing of the surfaces is the less diffuse process because of the difficulty on guarantee the original optical performances of the cover lens during all the mass production period. The deposition of the coatings on foils, e.g., in Roll-to-Roll (R2R) printing, is required for the main manufacturing technologies of display cover lenses.

2.3. Manufacturing technologies of automotive display cover lenses

In manufacturing scenarios, the experts have identified key technologies for the industry sectors such as improvement in reliability, control, measuring, precision and testing. Two main phases take place in the manufacturing chain. These are functional foil manufacturing such as R2R printing, bonding, curing, cutting, forming and packaging and over-moulding phases, in the case study in-mould labelling (IML), calendering and film lamination.

IML is a very robust method for decorating consumer and industrial products. IML gives product manufacturers the ability to have multiple colours, graphic effects and/or textures when the part comes out the mould. It is a cost-effective alternative to pad printing, hot stamping, paint and laser etching. IML has many advantages

over pressure-sensitive labels such as its ability to eliminate secondary operations and problems typically seen with an adhesive application. It offers a 'no-label' look and is more durable. Some of the technical advantages of IML include:

- Complete decoration of the moulded part
- Durability of graphics: Inks are protected by film in second surface constructions
- Secondary operations associated with post-moulding decoration are eliminated
- Abolition of need for recessed label areas
- Multiple films and constructions available to meet customer requirements
- Easier to produce multi-colour applications
- Generally lower scrap rates
- More durable and tamper-proof
- Superior colour balancing
- No area where dirt can collect
- Unlimited colours available

Instead of decorating parts with a common pad printing or painting, IML is done during moulding. The label is loaded into the mould, where it is fused into the outer surface of the moulded part. Figure 4 shows the IML manufacturing process. In mould labelled graphics are impervious to chemicals and abrasion. A sealed construction with inks on the top (first surface) of the label that bonds to the moulding, or inks on the back (second surface) of a clear material that traps inks between the label and the moulding, makes IML highly durable. To facilitate handling during printing and in production, the film must be of a certain stiffness [14].

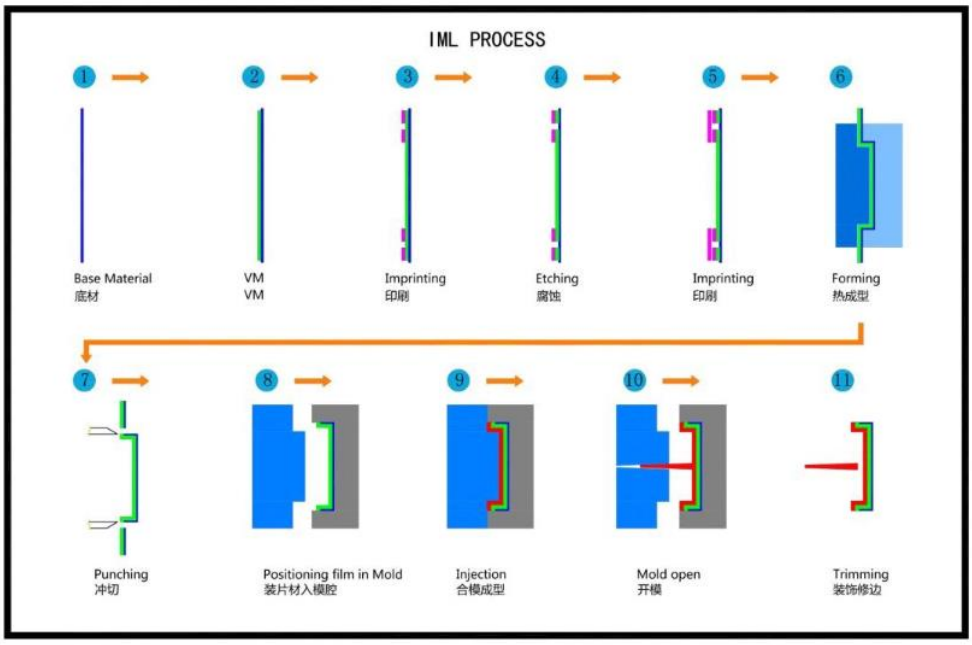

Figure 4: IML manufacturing process flow, broken down in separate process steps [15]

Use of the right film and correct printing as well as punching of the label are essential for a successful application of IML. In the interest of better adhesion and avoiding peeling, the label material must be identical with the container's material. However, combination between different plastic is also possible. Adhesion between different foils and over-moulding materials is in Table 1 reported.

Table 1: Adhesion between different foils and over-moulding materials.

		Over-moulded material		
		PC	PP	PMMA
Foil Material	PC	++++		++
	PET (certain)	++++	-	+
	PEN	+	-	-
	PP		++++	

++++ Excellent adhesion > 1.5 N, +++ good adhesion > 1 N, ++ fair adhesion > 0.5 N, + weak adhesion > 0.2 N, - no adhesion

Calendering is a speciality process for high-volume, high quality plastic film and sheet, mainly used for PVC as well as for certain other modified thermoplastics. The

calendering is a process of smoothing and compressing a material during production by passing a single continuous sheet through several pairs of heated rolls. Calendering is a final process in which heat and pressure are applied to a material by passing it between heated rollers, imparting a flat, glossy, smooth surface. The temperature and speed of the rolls influences the properties of the film. Calendering allows speciality surface treatments of the film or sheet such as embossing or enhancing the physical properties or in-line lamination. The main characteristics of the calendering process are reported in Table 2; in Figure 5, instead, the process scheme is illustrated.

Table 2: Main characteristics of calendering process [16]

Application	Cling film, vinyl, plastic bags, shrink-wrap, any plastic sheeting.
Advantages	High volume
Disadvantages	•Short to medium life • Flat and simple surfaces possible • Shrinkage can occur
Volume	• Large widths • High sheet and film quality • Adjustable thickness
Material	Thermoplastics such as: LDPE, cellulose acetate and PVC.
Cost	Lower cost with higher volume

Film lamination process is typically used in the manufacturing of display coverlens to apply a film with treatments, as AG coating, on glass substrate. The process of lamination consists of coupling two or more layers of PET film, polymers or other special materials and papers. The single layers are bonded to obtain a multi-layer laminate that sums the characteristics of each single material. The adhesives used for the lamination are developed specifically depending on the end use and convey to the laminate a chemical and thermal inertia as well as resistance to hydrolysis and UV rays.

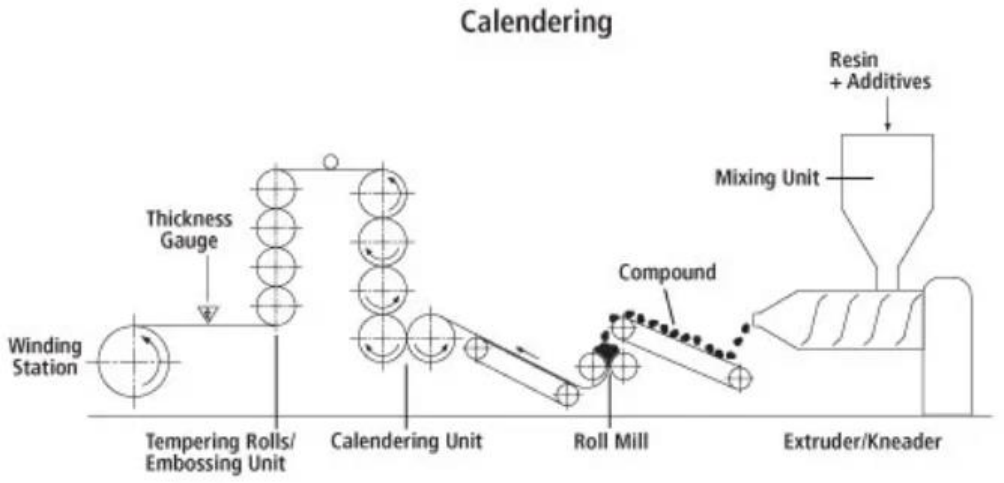

Figure 5: Calendering process scheme [17]

2.4. Transparent coatings deposition technologies

The presence of coatings on materials changes the properties of the surface and sub-surface region. Surface modification of materials allows for a variety of advanced properties, such as physical, chemical, electrical, magnetic, optical, mechanical, corrosion-resistant properties. The surface chemistry, morphology and mechanical properties could be important to further adhesion, film formation process and the resulting film properties [18]. Different techniques are used for the deposition of the coatings on the substrate surface:

- Chemical vapour deposition
- Physical vapour deposition
- Chemical and electrochemical techniques
- Spraying
- Roll-to-Roll coating processes
- Physical coating processes

In the next sections, a brief description of the more diffuse techniques used for display cover lenses are reported.

Physical vapour deposition (PVD)

PVD techniques are used in a wide range of applications, from decorative to high temperature superconducting films. PVD technologies can deposit a wide range of inorganic materials, including metals, alloys, compounds, and mixtures, as well as some organic materials, such as polymers. PVD is now used to create multilayer coatings, gradient depositions and extremely thick deposits.

PVD processes employ a variety of vapour phase technologies. In general, PVD refers to a variety of methods for depositing thin solid films onto various surfaces via the condensation of a vaporized form of the solid material. PVD involves the physical ejection of material in the form of atoms or molecules, followed by condensation and nucleation of these atoms onto a substrate (see Figure 6). The vapour phase material can be ions or plasma, and it is frequently chemically reacted with gases introduced into the vapour to form new compounds, a process known as reactive deposition. The thicknesses of the deposited layers can range from a few nanometres to thousands of nanometres [19].

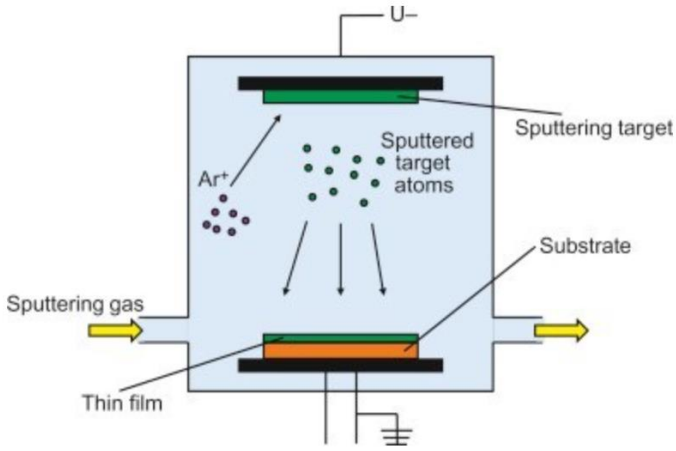

Figure 6: Physical vapour deposition scheme [20]

Three basic steps can define every PVD process:

1. Deposition or vapour-phase species generation: material can be converted to a vapour phase via evaporation, sputtering, or chemical vapours and gases.

2. Transport of the species to the substrate: vapour species can be transported from the source to the substrate using line-of-sight, thermal scattering, or molecular flow conditions (without collisions between atoms and molecules). Alternatively, if the partial pressure of the metal vapour and/or gas species in the vapour state is high enough to ionize some of these species (creating a plasma), many collisions will occur in the vapour phase during transport to the substrate.
3. Film deposition on the substrate: after the atoms or molecules have been deposited, the film nucleates on the substrate and grows through a variety of processes. By bombarding the growing film with ions from the vapour phase, the microstructure and composition of the film can be altered, resulting in sputtering and re-condensation of the film atoms and enhanced surface mobility of the atoms in the near surface and surface of the film.

All the processes are associated with two sets of parameters: plasma, which includes electron density, electron energy, and ion distribution, and process parameters, which include evaporation rate, gas composition, pressure, gas flow rate, substrate bias, and temperature.

The application of the PVD technique for the manufacturing of display cover lenses coatings is widely used for the deposition of inorganic coatings, such as anti-reflective or anti-fingerprint.

Roll-to-Roll coating processes: slot die coating

Slot die coating technology is a function of the coating process, auxiliary system, and fundamental technique for the application onto typically flat substrates such as glass, metal, paper, fabric, or plastic foils [21]. The decision to utilize a coating technology needs to be analysed against these functions to determine best fit. It is relevant in numerous commercial processes and nanomaterials related research fields as diverse as optical films to battery technology [22]. The desired coating material is typically dissolved or suspended into a precursor solution or slurry: the ink. It is delivered onto the surface of the substrate through a precise coating head known as a slot-die, as reported in Figure 7. By closely controlling the rate of solution deposition and the relative speed of the substrate, slot-die coating affords thin material coatings with easily controllable thicknesses in the range of 10 nanometres to 100's of micrometres after evaporation of the precursor solvent [23]. The most

relevant benefits of slot-die coating are thickness control, non-contact coating mechanism, high material efficiency, scalability of coating areas and throughput speeds, and roll-to-roll compatibility.

In the automotive display sector, this technology has become a critical process in the production of adhesive films, flexible packaging and LCD panels.

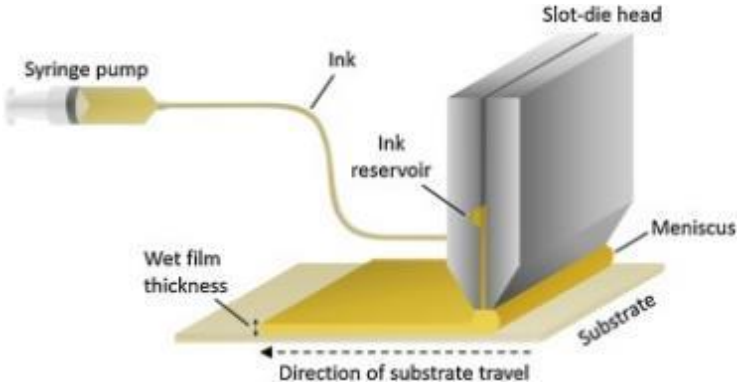

Figure 7: Slot-die coating process [24]

Flow coating process

Flow Coating involves spraying a component with excessive amounts of paint or lacquer or applying streams of the coating material to it. The excess coating material that drips off is then collected, filtered, and automatically reintroduced to the lacquering system [25], allowing no material loss occurs during the process. This technology provides several other interesting benefits when compared to other coating technologies. It is ideal for coating items with complex geometrical structures and allow the 100% of surface coverage. Moreover, flow coating is characterized by a high application efficiency and a uniform coating deposition. This process is widely used for the deposition of hard coat and anti-glare coating on the cover lenses surface.

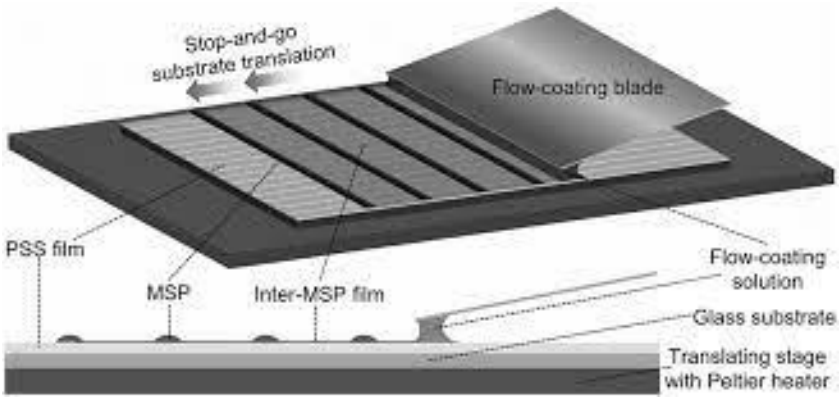

Figure 8: Schematic representation of flow coating process [26]

In Table 3 the main advantages and disadvantages for the described techniques are reported.

Table 3: Main advantages and disadvantages of transparent coating deposition technologies

Deposition technique	Advantages	Disadvantages
Physical vapour deposition	-Able to deposit a wide variety of metals, insulators, alloys and composites -Replication of target composition in the deposited films -Capable of in-situ cleaning prior to film deposition by reversing the potential on the electrodes -Reproducible deposition control -Sufficient target material for many depositions	-Substrate damage due to ion bombardment or UV generated by plasma -Deposition rate of some materials quite low -Some materials (e.g., organics) degrade due to ionic bombardment -Most of the energy incident on the target becomes heat, which must be removed

Slot die coating	-Extremely uniform film across large areas -Easily integrable into scale-up processes - Thicknesses ranging from a few nanometres to many microns	-Defects due to instabilities in the coating bead meniscus -Defects due to external factors either relating to the delivery of fluid, movement of the substrate, or the viscoelastic properties of the solution.
Flow coating	-Smooth flow-coat tunnel -Low quantities of paint and easy cleaning - easy on paint and high flexibility for changes of paint	-Wedge effect -Solvent reflux -Careful control of evaporation to obtain uniform coatings -Bubbling and foaming control for waterborne paints

2.5. Coatings for automotive display cover lenses

The presence of functional coatings onto the plastic or glass substrate is required for an automotive coverlens to improve mechanical and optical properties of the substrate materials:

- Higher resistance to mechanical stress, as scratch and wear
- Higher resistance to chemical substances, e.g., acids and cosmetic products
- Higher resistance to sunlight exposure, in particular UV (Ultraviolet) radiation exposure of plastic components
- Reduction of external light source reflection, to avoid the glaring of the driver
- Higher cleanability of the surface, e.g., fingerprint removal from the touch surfaces

In order to meet all the characteristics described before, one or more coatings can be deposited on the substrate surface: anti-reflective (AR), anti-fingerprint (AF), anti-glare (AG), hard coat (HC) or anti-microbial (AM). The mechanical properties of the material are typically evaluated to check if the desire performances of the coating are achieved. FCA (FIAT Chrysler Automobile) has developed an internal standard to investigate the reliability and robustness of the cover lenses [27]. In this standard, are reported the description of tests used to investigate the resistance of the coatings to chemical substances, the mechanical performances, e.g., wear resistance, and the reliability of cover lenses. Reliability of cover lenses is investigated by stressing the component in extreme climatic conditions: thermal cycles, humidity cycles and artificial weathering are an example of the tests performed.

The most important difference between an automotive display and other devices, such as smartphones, is the fixed position of the display inside the vehicle and the impossibility to change the display orientation in case of exposure of the device to external light sources. These conditions determine some undesired effects when the device is illuminated from an external light source, e.g., sunlight. The undesired effects are principally the less readability of the display screen and the glaring of the driver. To reduce the effects of external light exposure coatings, AR and AG coatings are used. These coatings have the functionality to decrease the intensity of specular reflection of external light.

The light reflected from the glass surface is, for normal incidence, approximately 4% of the incident light in the visible range; this value is determined by the refractive index of the glass (n_{glass} = 1.5) [28]. The application of functional coatings can determine in principle a reduction of specular reflection intensity up to 0.05%, respect to the initial intensity, in the visible range. How AR and AG coating determine a decrement of the specular reflection is described in Figure 9. Interference effects of thin layers determine the decrement of the specular reflection in AR coatings. This is obtained by modulating the refractive index of the coating [29]. AG coatings determine a decrement of specular reflection by diffusing the light in all the solid angle. This is obtained by means of nano-structured surfaces and/or the presence of organic or inorganic particles dispersed in the bulk resin [30]. The characteristics of AG coatings, the main materials under investigation in this work, are described in the following section.

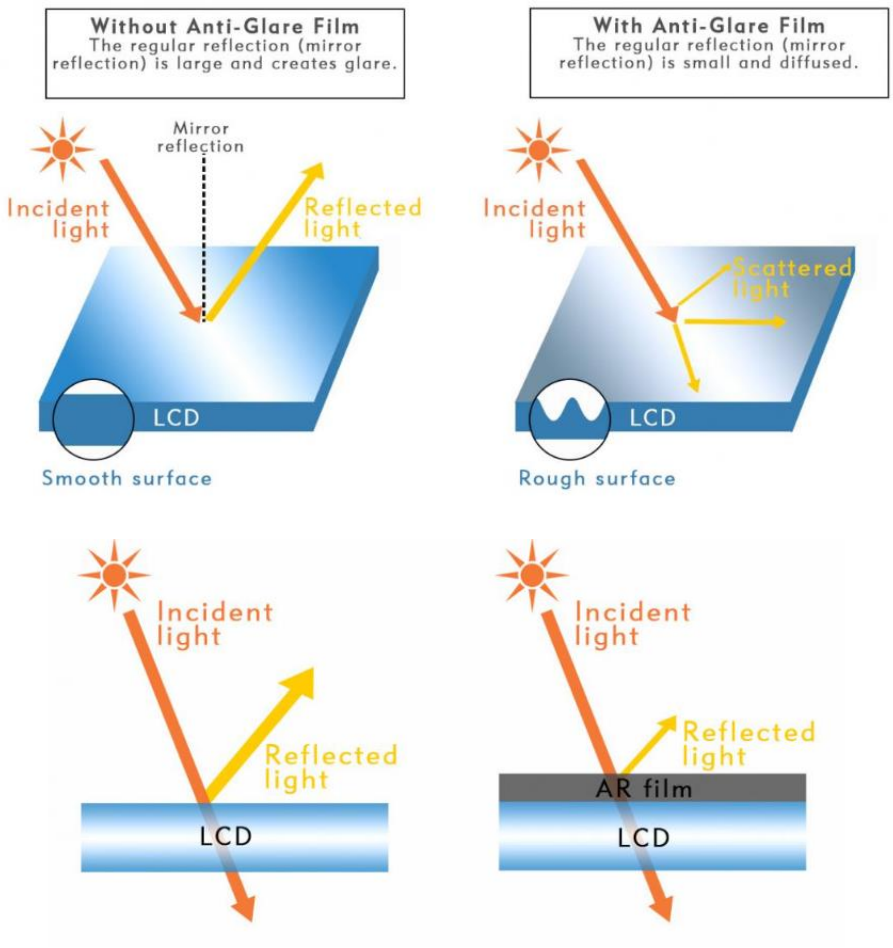

Figure 9: AR and AG coating decrement of specular reflection [*Errore. L'origine riferimento non è stata trovata.****]***

2.6. Anti-Glare coatings

Anti-glare treatment can reduce the light intensity and glare caused by excessive concentration of light, thereby improving the user's comfort for a cover lens. At present, surface roughening is the predominant route to prepare anti-glare thin films. The related methods involve particle blast, solution etching, solution spin/dip coating, spraying and imprint [31].

Typically, in the electronic display industries, for low-cost processing, the hydrofluoric acid (HF) solution-based is widely used for surface treatment of AG. However, the **chemical etching** technique has the disadvantage of lowering the durability of the glass due to the chemical reactions between the hydrofluoric acid and the composition materials in the glass. In addition, HF is a very hazardous chemical with very strong worldwide regulations.

Sandblasting or abrasive blasting is a physical–mechanical technique using fine particle type abrasives, which are accelerated through high-speed air or gas through a nozzle and then etched through a physical impact on a hard surface [33].

The **spraying** technique consists in a sol-gel solution sprayed onto a glass or plastic substrate. The materials were cured at high temperature (500°C in case of glass substrate, 130°C in case of plastic substrate) to roughen the surface in order to form an anti-glare coating. Additionally, in some techniques, spherical silica powder onto a glass substrate acts as a light scattering layer. However, this powder tended to aggregate with each other due to high surface energy, causing poor dispersion efficiency [31].

Spin coating is a simple method to create film on planar samples. The process starts depositing the dilution of the material in a solvent. This solution is subsequently dispended on the substrate surface. The substrate is the spun at high speed. Three parameters determine the thickness of the coating: speed, surface tension and viscosity of the solution [34].

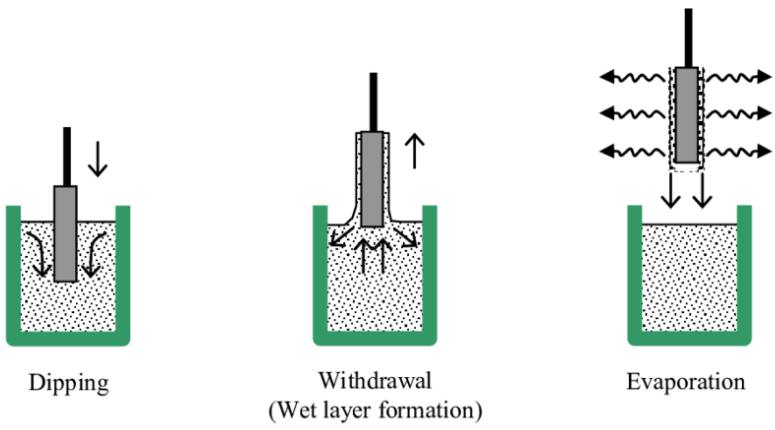

Figure 10: Dip coating process [35]

Dip coating process is described in Figure 10. Three main phases can be considered: the dipping of the substrate in the slurry; the wet layer formation and the solvent evaporation. The coating is generated during the wet layer formation. The thickness depends on multiple factors, as wettability, roughness, and porosity.

Independently from the fabrication technology, the AG coating is characterized from a rough surface. The roughness determines the scattering power of the incident light of the surface. At macroscopic level, the samples are considered illuminated at an angle of incidence with reference to the macroscopic sample normal.

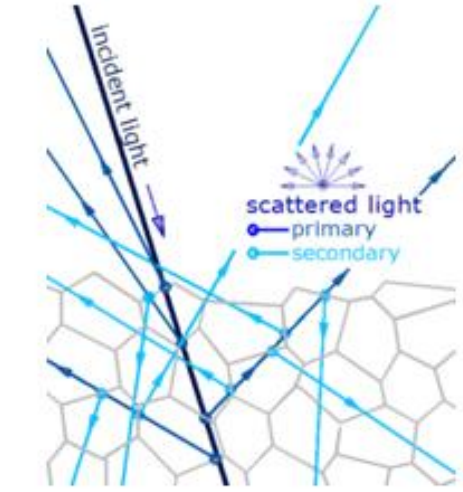

Figure 11: Description of light scattering on a rough surface

At the microscopic level, the roughness determines an illumination of the microscopic part of the surface at an angle with reference to the normal that is different from the neighbouring microscopic area, as described in Figure 11. The combination of the specular reflections of all the microscopic surfaces at a given angle determines the amount of the intensity reflection at that specific angle. In general, in the next sections, the specular reflection will be always considered at macroscopic level and diffusive reflection will be consider the light reflected at different angles with reference to the specular one.

The interaction between the light and the material under investigation has a direct relationship with some optical properties typically used in automotive sector: gloss and haze.

Gloss has been extensively used in the coating industry to describe the reflectance properties of a coating. It is one of the most important indicators used to describe the visual effect of an object [36]. It has been defined as the attribute of surfaces that causes them to have a shiny or glossy, metallic appearance. The gloss of a surface can be greatly influenced by several factors, for example the angle of incident light and surface topography, the smoothness achieved during polishing, the amount and type of coating applied or the quality of the substrate [37].

The specular gloss is defined as a measure of the specular reflectance of a surface relative to the initial intensity of the light source at a well-defined angle of incidence θ:

$$G\ (GU) = 100 * \frac{I(\theta)}{I_0(\theta)},$$

(2. 1)

where I(θ) is the intensity of specular reflection of the sample; $I_0(\theta)$ is the incident light intensity. The angle θ could be 20°, 60°, or 85° [38]; the angle selection depends on the sample finishing:

- 85° → matt surface (gloss level ≤ 10 GU)
- 60° → mid gloss (10 < gloss level < 70 GU)
- 20° → high gloss (gloss level ≥ 70 GU)

Haze gives the percentage of transmitted light that deviates from the incident light beam [39]:

$$H\ (\%) = 100 * \frac{T_{diff}}{T_{tot}},$$

(2. 2)

where T_{diff} is the transmitted diffuse light, T_{tot} is the total transmitted (direct + diffuse) light.

Haze can be the result of the moulding process or of the surface texture. There are several factors responsible for light scattering such as surface roughness and internal optical irregularities caused by crystallization or material's level of crystallinity. Note that a reduction in haze not necessarily leads to improved clarity. Haze due to surface roughness is in many cases inversely related to gloss [40].

The relationship between gloss and surface parameters was investigated in the study of Q. Yong et al. [38]. In that work, a linear relation was demonstrated between gloss and the surface parameters S_a and S_q, as reported in Figure 12.

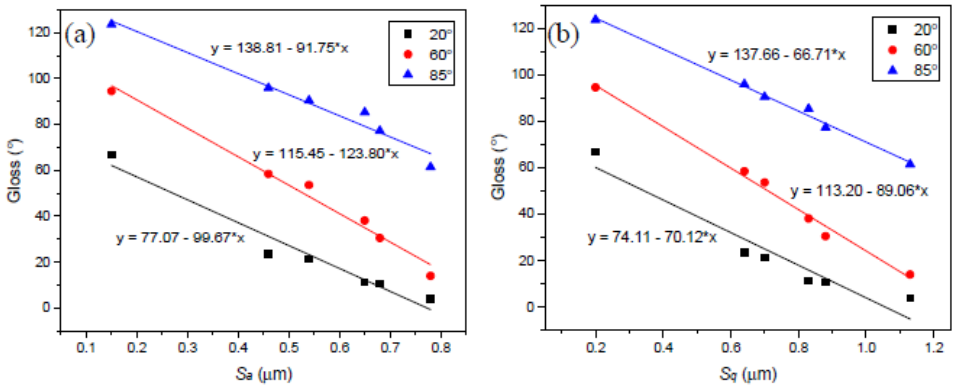

Figure 12: Gloss as a function of surface roughness (a) S_a and (b) S_q calculated from 5000 µm x 5000 µm images

The parameters S_a and S_q are areal field parameters. The field parameters account for the vast majority of surface texture parameters and can be used to characterize surface heights, slopes, complexity, etc. They are defined in the specification standard ISO 25178 [41].

S_a, the Arithmetic Mean Height, is the arithmetic mean deviation of the roughness evaluated over the calculated 3D surface.

$$S_a = \iint_a |Z(x,y)| d(x) dy$$

(2. 3)

S_q, the Root Mean Square Height, is defined as the root mean square deviation of the roughness evaluated over the calculated 3D surface.

$$S_q = \iint_a (Z(x,y))^2 d(x)dy$$

(2. 4)

The S_a and S_q parameters are highly correlated with one another. The S_q parameter has greater statistical significance (it is the standard deviation) and is often more physically grounded than S_a; for example, S_q is directly related to surface energy and how light is scattered from a surface.

Specular gloss and surface roughness are important factors of coatings as they influence the visual perception of a coating on products [42]. In the case study, it is important to investigate how the presence of AG coating on display cover lenses affects the readability of the display. The principal effects due to the presence of this kind of coating is **lower clarity, blur and generation of sparkle effect**.

The core activity of this thesis is the evaluation and the quantification of these phenomena, with a special attention to sparkle effect quantification. Sparkle effect will be deeply described in chapter 4.

2.7. Conclusions

This section described the principal characteristics of an automotive display, which is its structure, and which are the materials used for the manufacturing of the different parts of the component. It was also described which are the coating deposition techniques and the main techniques for the manufacturing of display cover lenses. A particular attention was dedicated to the description of AG coatings, the principal material used on top of display cover lenses investigated in the next sections. In the description of this coating were explained the principal optical characteristics and the correlation between gloss and haze with the height parameters extracted from morphological analysis. The same optical parameters can be used for the assessment of **AR coatings.**

3. Methodologies for material validation

In this section, the methodologies used for the assessment of the materials for automotive display applications are described.

3.1. Introduction

In literature, there are not well-defined standards for the whole assessment of an automotive display cover lens. For these reasons, in the next paragraphs are collected all the main methodologies for the optical properties' evaluation of cover lens. The methodologies described are extracted from international standards, from research studies and from CRF internal standards. The final goal of this section is to express good display cover lenses metrology in an unambiguous manner and to present measurement methods clearly and in a self-contained way.

In particular, it is provided a description of:

- methodologies for **aesthetical and surface finishing of materials**, i.e., gloss unit evaluation and haze quantification
- methodologies for the assessment of the morphology of display cover lens
- techniques used for the quantification of **display** optical output variation due to the **interaction with the materials** used for the display cover lenses.

The **aesthetical and surface finishing** of the materials used for display cover lenses is evaluated with different optical techniques. The principal methodologies used in this work are:

1. **Gloss Unit** (GU) detection
2. **Haze** evaluation
3. **Luminous transmittance and reflectance** of the materials
4. **Morphological** analysis

More details on the instrumentation and the techniques used for the evaluation of these parameters are reported in Annex A.

3.2. Assessment of optical interaction of the cover lenses materials with display light source: experimental method

In this paragraph, the methodologies applied to characterize the whole automotive display system, comprising the coverlens bonded to the display with optical and mechanical functional coating on top are described. The characterization allows the detection of optical performances, the materials interaction with the light source and the quality of the images.

The optical parameters under investigation are:

- Luminance of full screen white and black
- Contrast Ratio
- Uniformity
- Colorimetric coordinates
- Defect analysis, e.g., sparkle effect, bubbles, stains, and cracks

The tests are performed in a **darkroom** in order to avoid ambient lighting, reflections and light diffusion that can affect the measurements. The darkroom has less than 0.01lx falling upon the screen.

The complete optical characterization described in this section requires the use of different test instruments because one single luminance meter/colorimeter cannot perform all the tests with the desired accuracy:

- **Array detectors** (or luminance cameras) can capture the entire display screen in one image. It is composed of an array of sensors (e.g., a CCD) coupled with an optical lens. An array detector is necessary for uniformity measurements and the detection of defects, but it is usually less accurate. An array detector must be carefully calibrated by considering different sources of errors: pixel non-uniformity and lens cosine fall-off. Moreover, it is sensitive to the Moiré effect that must be avoided and or eliminated.
- **Spot detectors** can perform luminance/colour measurements at one single point of the display at a time. It is a light sensor coupled with an optical lens with a fixed angle of acceptance. It is usually quite precise and easy to use but it is not suitable for uniformity measures. Moreover, the actual field of view of the instrument can greatly affect the results.

The Moiré effect is an undesirable visible luminance modulation, which has a spatial variation usually substantially larger than the pixel-to-pixel separation. Moiré effect creates an artefact that affects the uniformity measurement and must be removed before processing the image.
This can be achieved by:

1. defocusing the lens until the Moiré modulation disappears from the collected image. Defocusing can be easily implemented but leads to a loss of resolution.
2. applying a digital low-pass filter
3. orienting the device correctly respect to the detector. The x and y-axis of the device must be parallel to the x and y-axis of the array detector.

Typical specification of the two kinds of instruments is following reported:

- **Luminance/colorimeter array detector:**
    1. Minimum wavelength range: 380-780nm
    2. Minimum Luminance: 0.05Cd/m2
    3. Maximum Luminance: 10000Cd/m2
    4. Luminance accuracy: ≤3%
    5. CCD pixel number no lower than Device under test (DUT)
    6. Dynamic range >100.000:1
- **Spectroradiometer/colorimeter spot detector**:
    1. Minimum wavelength range: 380-780nm
    2. Minimum Luminance: 0.05Cd/m2
    3. Maximum Luminance: 10000Cd/m2
    4. Luminance accuracy: ≤3%
    5. Chromaticity accuracy: less than ± 0.005 for standard illuminant A
    6. Measuring angle ≤1° (the measuring angle of the detector should be changeable if necessary)

The optical characterization of the devices in this work is performed by Radiant PMI16-XB CCD (Charge Coupled Device) colorimetric camera (Figure 13) and Konica Minolta CS-2000 spectrophotometer.

Figure 13: Radiant PMI16-XB colorimetric camera

The Radiant camera can determine photometric quantities as luminance and colorimetric coordinates. The colorimetric coordinates are defined in the CIE XYZ 1931 colour space. The coordinates X, Y and Z identify the three primary imaginary colours because the saturation levels are such as not to be detected from human retinal photoreceptors. The X coordinate show two peaks wavelength at 450nm and 600nm, whilst the peak wavelength of Y and Z coordinate are respectively at 520nm and 477nm. CIE XYZ colour space is defined on the spectral response of the photoreceptors of the human eye. The three functions, called colour matching functions represent the human eye response are $\bar{x}(\lambda)$, $\bar{y}(\lambda)$ and $\bar{z}(\lambda)$. The Radiant camera determines the colorimetric coordinates with the aid of filters with a spectral response comparable with that of the colour matching functions of CIE 1931. The graph in Figure 14 shows the spectral response of the filters.

The main parameters of the Radiant camera are reported in Table 4.

Table 4: *Selectable parameters of Radiant PMI16-XB colorimetric camera*

Parameter	Value
f/#	3.3 or 8.0
Exposure time	0-60000ms
Minimum focusing distance	0.310m
Max image resolution	4896x3264px
High dynamic range	T/F
CCD working temperature	5°C

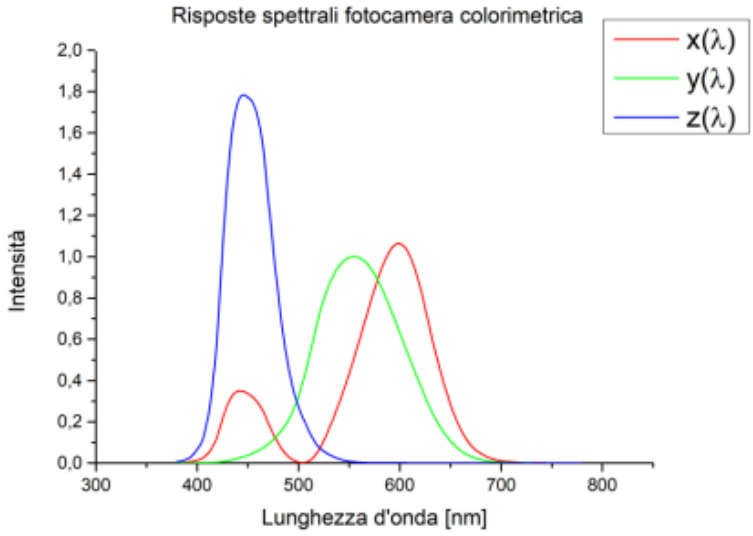

Figure 14: Spectral response of the filters [45]

The output provided by the camera is an image in luminance scale of the whole active area of the sample. The images are correlated to an NxM pixel matrix. Every pixel is associated to three values of the tristimulus functions XYZ. Starting from these values, the instrument can provide the colorimetric coordinates of the other colour spaces derived from CIE XYZ 1931.

Figure 15: Konica Minolta CS2000 spectroradiometer

The CS-2000 spectroradiometer (Figure 15) is a spot detector. It measures the spectral distribution of the source. The electromagnetic radiation emitted by the

source is optically collected by the objective; at this point the light passes thought a monochromator that determine the selection of narrow bands of wavelength. The acquisition range is 380 – 780nm by step of 1nm. The acquisition spot angle is selectable at 2°, 0.2° and 0.1°. The instrument also provides the CIE Lxy colorimetric coordinates and the luminance of the analysed spot.

3.3.1 Optical setup and alignment

Let consider a right-handed X Y Z Cartesian coordinates system with origin at the centre of the screen. The Z-axis is perpendicular (normal) to the screen, the X-axis is the screen horizontal, and the Y-axis is the screen vertical. The X and Y-axes lie in the plane of the display surface (Figure 16).

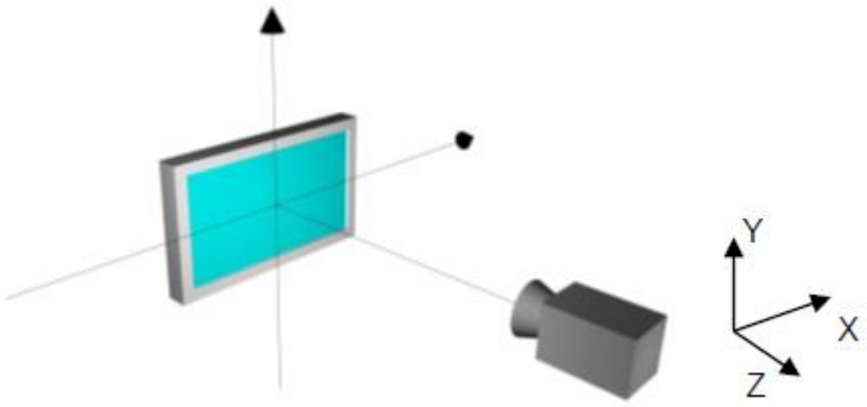

Figure 16: Experimental setup for display characterization

The display is aligned to have the X-axis parallel and the Y-axis perpendicular to the ground plane. The instrument is placed in front of the display at distance ***d***. The normal viewing distance of an automotive display is between 50 and 100 mm depending on the application. It would be reasonable to place the detector at a distance from the device that matches the normal viewing distance. Nevertheless, the instrument usually does not match the visual properties of the human eyes like min/max focusing distance, angular resolution, and field of view. Moreover, the luminance measurements are independent from the distance (for an extended homogeneous surface). Therefore, the measurement distance can be set to get the desired resolution and reproducibility. For an array detector, *d* should be enough to collect entirely the image of the display surface and to have more than one camera

pixel for display pixel; for a spot detector, *d* should be set to get the desired measurement field on the display surface.
Spot size detectors have a fixed or selectable measuring angle that intercepts the display. Depending on the measuring angle **α** and the distance *d* (see Figure 17), a specific measurement area is defined on the display surface (eq. (3. 1)). The measurement field has a diameter:

$$D = 2 * d * tg(\frac{\alpha}{2})$$

(3. 1)

Defects and non-uniformities smaller than the measurement area cannot be resolved. Consequently, the use of different measurement fields can lead to different results especially for not uniform displays.

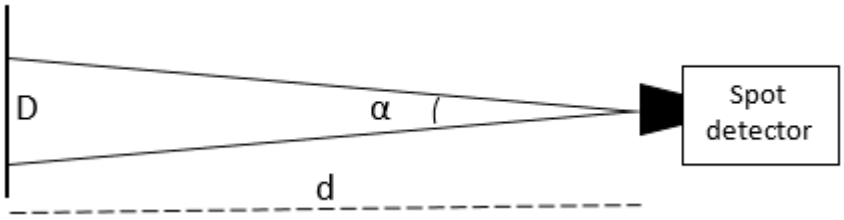

Figure 17: Experimental setup with spot detector device

The optical axis of the detector lens must be perpendicular to the display surface, pointing to its centre. A precise alignment is obtained by using a cross pattern reported. That pattern allows the camera image to be correctly centred and any tilts can be easily recognized by staircase effects of the white lines.

3.3.2 Test description and execution

The optical characterization is focused on measuring luminance, colorimetric coordinates, uniformity, and contrast ratio.
Luminance is a photometric measure of the luminous intensity per unit area of light travelling in a given direction. It describes the amount of light that passes through, is emitted from, or is reflected from a particular area and falls within a given solid angle [46]. The luminance of a specified point of a light source, in a specified direction, is defined in eq. (3. 2):

$$L_v = \frac{d^2 \Phi_v}{d\Sigma \, d\Omega_\Sigma \cos \theta_\Sigma}$$

(3. 2)

where:

- L_v is the luminance (cd/m2),
- $d^2\Phi v$ is the luminous flux (lm) leaving the area dΣ in any direction contained inside the solid angle $d\Omega_\Sigma$,
- dΣ is an infinitesimal area (m2) of the source containing the specified point,
- $d\Omega_\Sigma$ is an infinitesimal solid angle (sr) containing the specified direction,
- θ_Σ is the angle between the normal n_Σ to the surface dΣ and the specified direction.

In this work, luminance is evaluated on full screen for white and black patterns by an array detector, following FCA standard 7.M0015 [47].

3.3. Conclusions

The methodologies described in previous paragraphs are extracted from international standards, from research studies and from CRF internal standards. The final goal of this section was to express display cover lenses metrology in an unambiguous manner and to present measurement methods clearly and in a self-contained way. It was provided a description of methodologies for aesthetical and surface finishing of materials and techniques used for the quantification of display optical output variation due to the interaction with the materials used for the display cover lenses. The only methodologies not reported in this section are related to evaluation and quantification of sparkle effect, for which is dedicated a separated section (see chapter 4).

4. Use of polarization to evaluate the sparkle effect of materials

In this section, the description and the definition of sparkle effect will be provided. It will be investigated the current methodologies for the assessment of this effect and the description of a novel methodology characterized using polarized light is proposed.

4.1. Introduction to sparkle effect

S**parkle effect** (see Figure 18) is a transmission artefact where the displayed image appears to be covered by small, coloured highlights that scintillate with the relative movement of the display and observer [49]. The effect is mainly due to the light interaction with inner particles and microstructures at the surface as well. The presence of sparkle effect is related to the use of anti-glare coating on the top of the display coverlens.

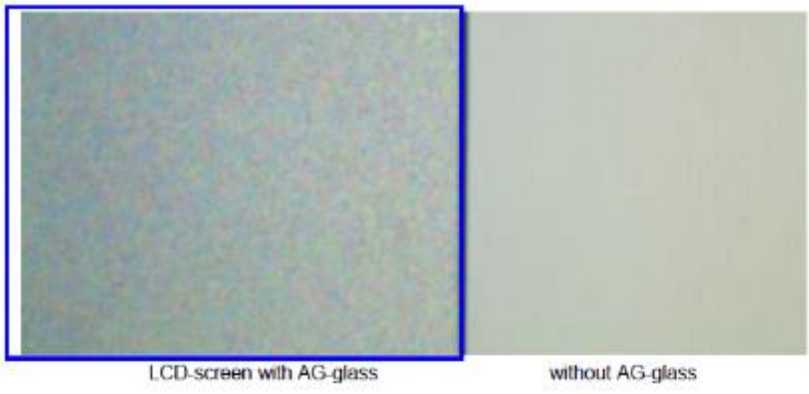

Figure 18: Sparkle phenomenon. Left display with anti-glare. Right display without anti-glare film [49]

Recently, several researchers have attempted to quantify the sparkle effect and to relate it to the physical properties of AG surface treatments. Some studies evidence the similarity in appearance between sparkle and speckle patterns. These last patterns are seen when coherent laser light is transmitted by diffusing surfaces. Concluding that sparkle has the same cause as laser speckle, Cairns and Evans [50] suggest that a useful measure for the characterization of sparkle is the standard speckle contrast (SC) function:

$$SC = \frac{\sigma_i}{I}$$

(4. 1)

where I is the transmitted intensity and σ_i is the standard deviation of the transmitted intensity over the measurement region.

4.2. Detection of sparkle effect generated by the application of Anti-Glare materials

Different methods are proposed for the quantification of sparkle effect. Becker and Neumeier [49] suggest placing camera and display at a specific distance to get 5-7 camera pixels per display sub-pixels (RGB) and displaying a uniform green image on the screen. They propose two methods to characterize sparkle: difference method and spatial filtering method. In the difference method, a first image is recorded and then the AG-glass is slightly shifted laterally before a second image is recorded. The difference between the two images eliminates the constant intensity levels and reveals the intensity variations produced by the AG surface (see Figure 19).

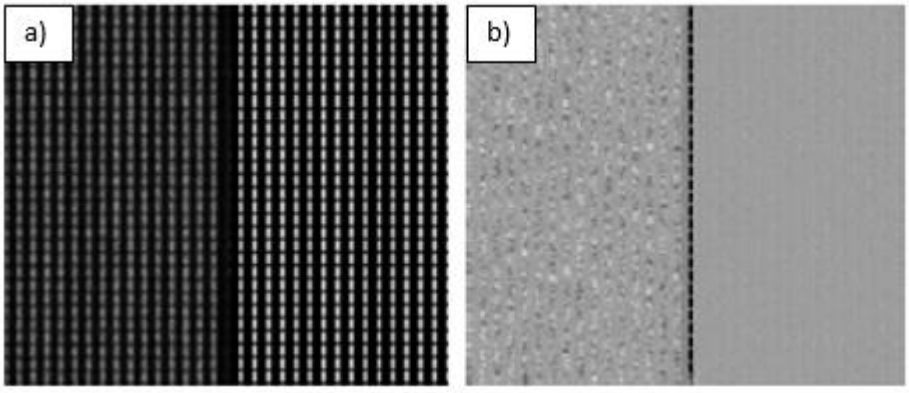

Figure 19: Differential method proposed by Becker and Neumeier: a) image of AG-layer on top of display surface covering half of the region of interest (left half). The right half is the bare LCD-screen; b) Regular intensity modulations removed by image subtraction. Sparkling becomes obvious in the left half of the image [49].

The spatial filtering consists in recording one single image. The intensity variations are computed by dividing the measured image values by a low pass filtered (averaged) version of the same image. This last technique may be advantageous if no mechanical interference (shifting of the AG-layer) is required.

Gollier et al. proposed a second method for the quantification of sparkle effect by means of pixel power deviation (PPD) [51]. They have developed the measurement device illustrated in Figure 20. In the device, the sample is placed at fixed distance from the display. The display is set to show a uniform green screen. The light transmitted by the sample is imaged on a monochrome CCD (charge-coupled device) camera through a pair of lenses (L1 and L2) and is stopped by a diaphragm (D) with aperture set to 12mrad to mimic the acceptance angle of the human eye. The optics are designed so that each LCD pixel is sampled by approximately 20 × 20 CCD pixels. The PPD of a given sample is calculated from images: firstly, the contribution from the display alone, without AG, is evaluated and set as the reference measurement. Then, a second image of the test sample containing the AG surface is collected. Finally, the PPD is calculated by means of mathematical algorithm.

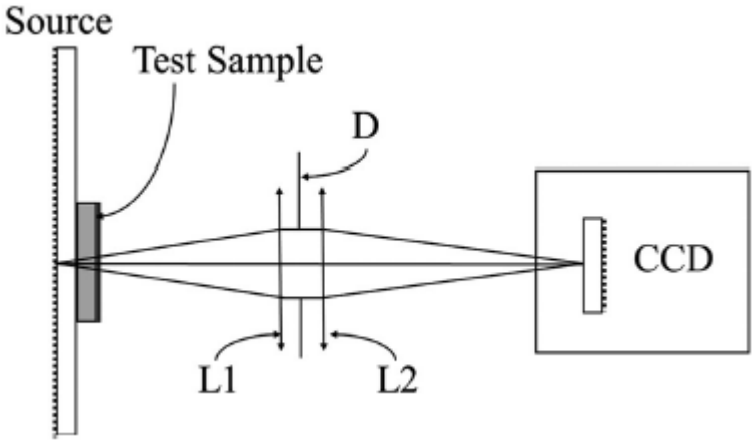

Figure 20: Diagram of pixel power deviation measurement device [51].

A third method is described from FCA internal standard 7.M0015 [47].

The main issue related to the use of all these methods is that it is not possible to separate between sparkle and Moiré effect contribution. The Moiré effect is a well-known phenomenon that occurs when two or more images with periodical or quasiperiodic structures (such as dot screens, line gratings, etc.) are combined to create a new superposition image [52]. An example is illustrated in Figure 21. In the case study, the two structures are represented by the array pixel of the display and the array pixel of the digital camera. The presence of the Moiré effect can affect the analysis of the images collected for the quantification of sparkle effect. In fact, both Moiré and sparkle effect determine a variation of the luminance. For this reason,

the assessment of the sparkle effect (see eq. **Errore. L'origine riferimento non è stata trovata.** is affected by the presence of Moiré effect.

Other important considerations are the difficulty to properly align the camera detector and the device under testing, the impossibility to eliminate the contribution of the luminance modulation of the display pixels and the impossibility to characterize independently from the light source the contribution of the cover lens. Moreover, due to the necessity of a fine alignment all these techniques are not easily applicable for analysis directly on the vehicle. The consideration of all these aspects have determine the necessity to develop a new system for the quantification of sparkle effect.

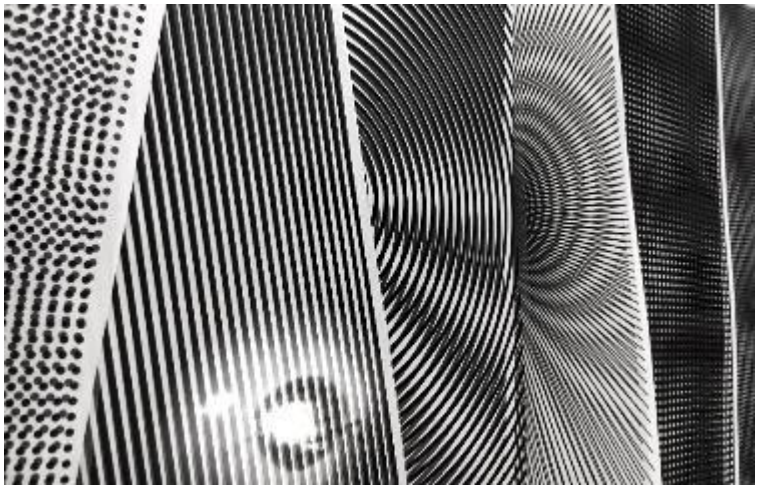

Figure 21: Example of Moiré effect [53]

4.3. Development of novel technique for the detection of sparkle effect by polarized light

During the PhD activity, an innovative methodology was developed to detect the sparkle effect due to the optical properties of the anti-glare coatings and the interaction with the light source, e.g. LCD display. This new method allows to analyse the distribution of the particles (precursors of sparkle effect) dispersed in the AG coatings giving fast response of the sparkle effect.

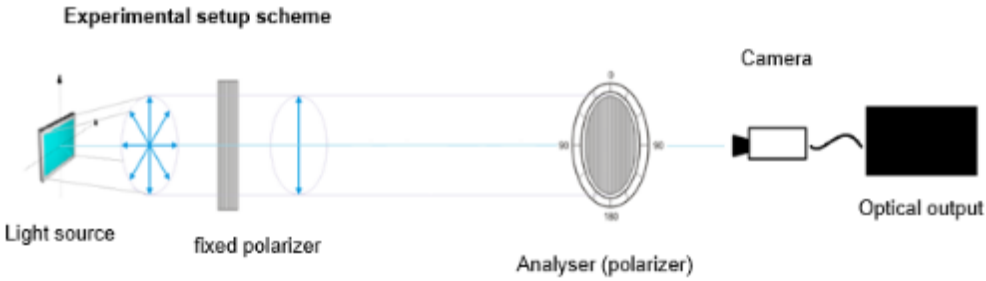

Figure 22: Experimental setup scheme for sparkle effect detection without AG material

The unpolarised light emitted to the light source goes through a first ***polarizer,*** as described in Figure 22. A second movable polarizer, the ***analyser***, is placed with the optical axes orthogonal to that of the first polarizer. Thus, the system is working in dark field. The light is finally collected by an array detector camera.

When the AG material is placed between the two polarizers, the light interacting with the sample changes its polarization direction in the points of the AG material in which the sparkle effect occurs. The resultant image is a dark background with bright dots (Figure 23).

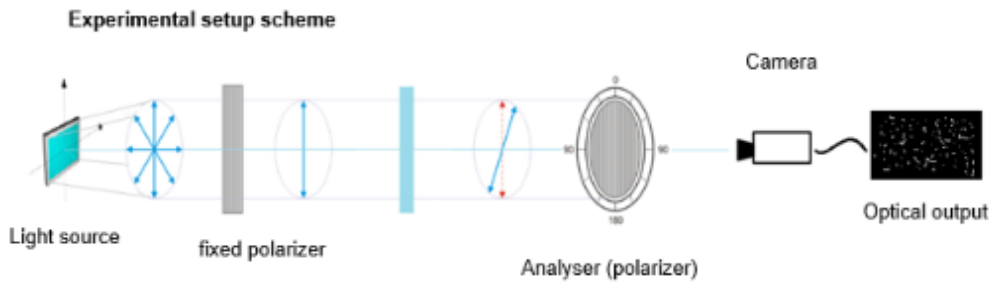

Figure 23: Experimental setup scheme for sparkle effect detection with AG material

Currently no other similar methods for detection of sparkle effect generated by AG materials are present on the market; for this reason, the acquisition method described was patented [54]. In Figure 24, the measurement setup in which the light source is a white LED lamp with a diffuser on top is illustrated. In the following sections, for some acquisitions alternatively to that LED lamp, an LCD display will be used as light source.

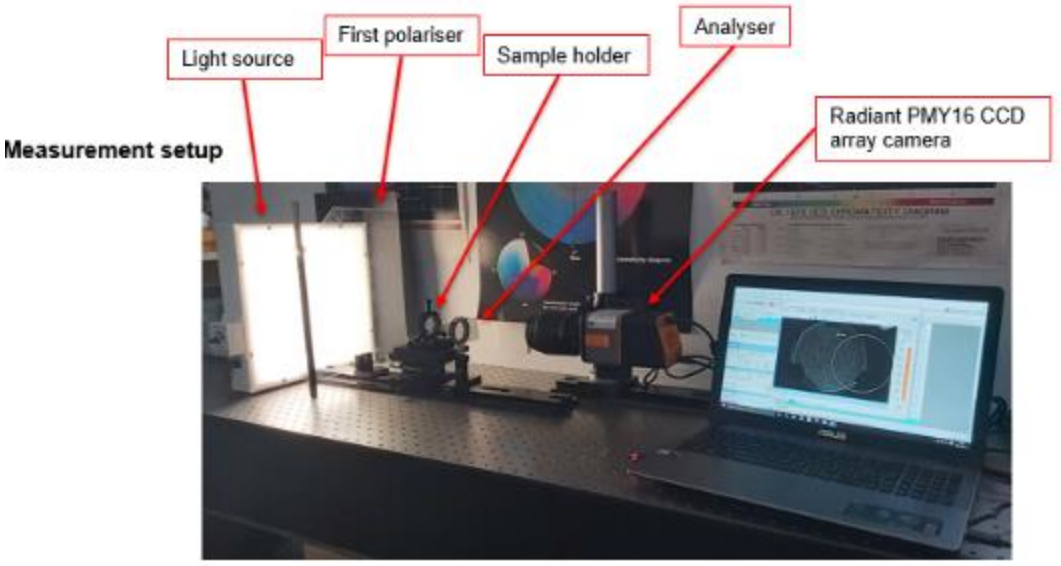

Figure 24: Experimental setup scheme for sparkle effect detection

Figure 25 shows the real appearance of the sample observed through the polarizers.

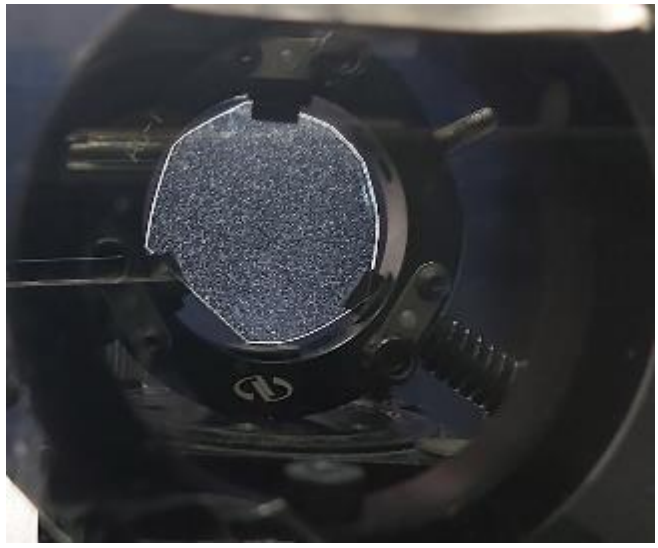

Figure 25: AG material appearance observed through the polarizers

4.3.1 Comparison of acquisition results with and without polarizers

The analysis of LCD display with array detector camera allows discerning the single emitting pixel or subpixel. The light emitted from the pixels has an average luminance higher than 600 cd/m^2 (for an automotive display) and a peak luminance in correspondence of the pixels higher than 1000 cd/m^2. These values of luminance determine a difficulty in discerning eventual defects from the subpixel. Figure 26 shows a comparison of two images of an LCD display collected without (a) and with (b) the material solution with an AG treatment on top.

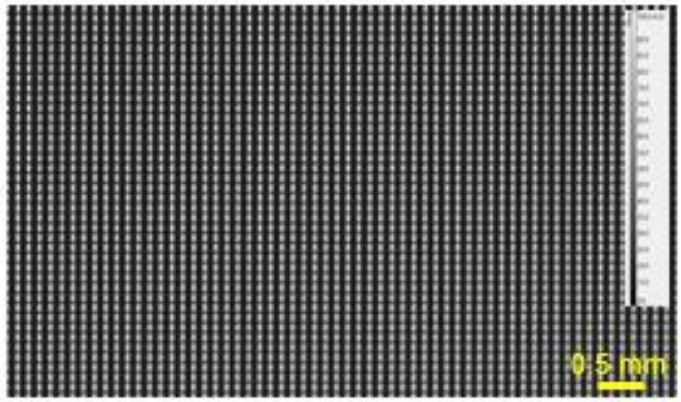

a)

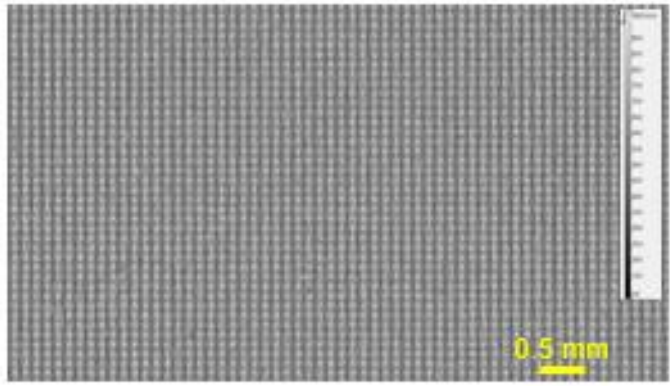

b)

Figure 26: a) LCD display optical output without AG material; b) LCD display optical output with AG material

The presence of coverlens with AG treatment determines a difference in perception and quality of the image. As noticeable in the Figure 26, by applying the coverlens, the grid of the pixels becomes less defined and clear referred to the acquisition without lens. Anyway, the analysis and the comparison of the acquired images is affected to the presence of luminance spikes of the pixels.

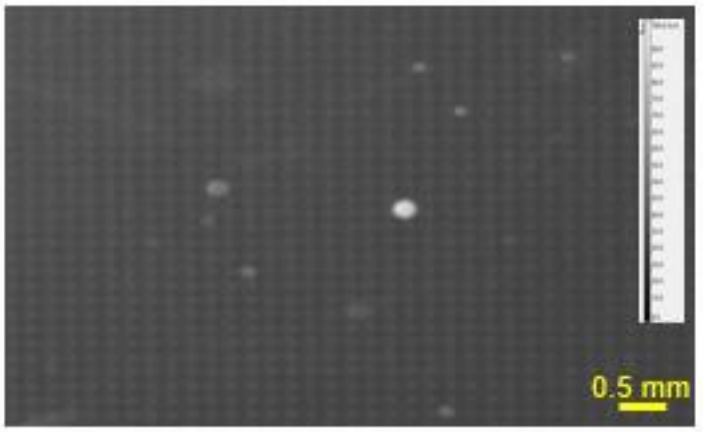

a)

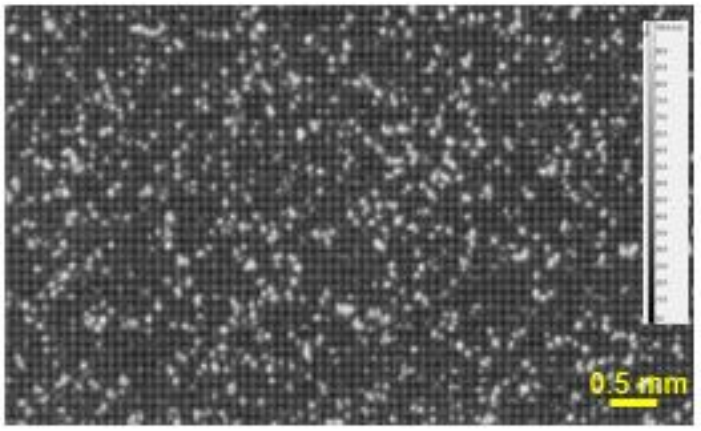

b)

Figure 27: New technique acquisition: a) LCD display optical output without AG material; b) LCD display optical output with AG material

The new methodology, described in the paragraph 4.3, allows minimizing the contribution of pixels. It is not feasible to eliminated at all the contribution because of the not ideality of the polarizers: as noticeable in Figure 27a, the light transmitted in dark field (optical axis of polarizers orthogonal) is not zero

By placing the coverlens with AG treatment in between the polarizers, the light changes its polarization status after the interaction with the inclusions and the surface of the AG treatment (Figure 27b). These points are brighter than the pixels' grid of the LCD (or brighter than the background in case of diffuse light source). This allows localizing the points in which sparkle effect occurs and analysing the acquired images. The analysis of the distribution of the spots and their density is correlated to the amount of the sparkle effect when the display is switched-on.

4.3.2 Image analysis for sparkle effect quantification

4.4. Conclusions

In this section, the description and the definition of sparkle effect was provided. An overview of the current methodologies for the assessment of this effect was proposed and the main issues in the application of these methodologies were described. They are related to the impossibility to distinguish between sparkle and Moiré effect, the difficulty to properly align the camera detector and the device under testing, the impossibility to eliminate the contribution of the luminance modulation of the display pixels and the impossibility to characterize independently the contribution of the cover lens. Moreover, due to the necessity of a fine alignment all these techniques are not easily applicable for analysis directly on the vehicle. All these aspects have determined the necessity to develop a new system for the quantification of sparkle effect. The new methodology is characterized using polarized light and allows identifying the area of the surface of the cover lens that generates the sparkle effect. The images collected with this technique were following analysed. The correlation of the analyses with the generation of sparkle effect is described in the following section.

5. Assessment of cover lenses materials

In this section, an introduction on the commercial samples used for the analysis is reported together with a description of the main results of the assessment of the materials. The results of the materials characterization of the commercial samples are also provided; in detail, for the purpose of this activity, it is most relevant the composition of the anti-glare coating (AG), information that is not provided by the supplier of the coatings.

5.1. Commercial samples under testing

The commercial samples used for the analysis are plaques or display cover lenses with Hard Coat (HC) and AG treatments on the top surface. The sample technology is described in the section 2.3 and reported in Table 5 for each component. The substrate of the samples can be inorganic, i.e., glass, or organic. The polymer used as substrate for display coverlens are typically Polycarbonate (PC), Poly Methyl Methacrylate (PMMA) or a combination of the two (PMMA/PC/PMMA). In the Annex B, more details on the samples under investigation are reported.

Table 5: Commercial samples under investigation

Sample	Technology	Substrate	Coating	Optical finishing
1	IML	PC (4mm)	HC + AG (8µm)	18.6 ± 0.4
2	Calendering	PC/PMMA/PC (2mm)	HC + AG (8µm)	21.9 ± 0.2
3	IML	PC (4mm)	HC + AG (8µm)	33.3 ± 0.7
4	IML	PC (3mm)	HC + AG (15µm)	40.0 ± 1.1
5	IML	PC (4mm)	HC + AG (8µm)	68.5 ± 1.9
6	IML	PC (4mm)	HC + AG (8µm)	75 ± 2
7	IML	PC (4mm)	HC (20µm)	85.7 ± 0.9

In the Table 5, the optical finishing of the samples is reported as Gloss Unit (GU) value (see paragraph 2.6). The values reported have been measured in laboratory with the Rhopoint Dual gloss IQ gloss meter at 60° for all the samples, except for sample 6 and 7 for which the measurement at 20° was selected. The uncertainty related to each value is the standard deviation calculated on five gloss measurements. These values are to be compared with those declared by the suppliers and shown in Table 15. The values obtained for sample 1 and 5 are higher than these declared by the supplier, whilst gloss values of sample 2 and 3 are lower. For the other samples, the results obtained are in accordance with the values declared by the suppliers.

5.2. Optical properties of the materials

The samples under testing have been optically characterized in terms of luminous transmittance, reflectance and haze as described in Annex A. The transmittance and reflectance spectra are the average of different measurements collected on different specimens of the samples.

The last optical properties investigated in this paragraph is the Haze. It is defined as the percentage of transmitted light that deviates from the incident light beam. High values of Haze are typical of materials with low clarity. In Table 6 the results obtained for the samples under testing are reported. The uncertainty of haze values is the standard deviation of five measurements. The presence of the AG treatment determines an increment of the haze with respect to the solution (sample 7) that is characterized by the presence of the only HC treatment.

Table 6: Haze values of samples under investigation

Sample	Haze (%)
1	10.5 ± 0.4
2	12.7 ± 0.1
3	9.5 ± 0.6
4	10.3 ± 0.1
5	2.7 ± 0.3
6	1.61 ± 0.14
7	0.30 ± 0.02

5.3. Materials characterization

The materials compositional and morphological characterization is a necessary step to relate the different properties of the samples under analysis to the materials involved. The solutions are commercial products; for this reason, the materials used for the manufacturing of the samples are not available, with the only exception of the substrates. The optical properties of AG coatings are obtained by means of nano-structured surfaces and the presence of organic or inorganic particles dispersed in the bulk resin. The resin determines an increment of adhesion and a homogeneous dispersion of the particles in the surface. Typically, silica/acrylate systems or waterborne polyurethane are used. Two different techniques were used:

- Fourier Transform Infrared spectroscopy (FTIR) is used in this work to determine the nature of the bulk resin of the coatings.
- Energy Dispersive X-Ray Spectrometry (EDS), used to identify the composition of the inorganic particles eventually dispersed in the bulk resin. Moreover, the EDS technique allowed correlating the results obtained with the presence of the dispersed particles.

5.3.1. Fourier Transform Infrared spectroscopy (FTIR)

FTIR spectra were obtained by acquisitions in ATR mode (Attenuated Total Reflection mode) on diamond crystal.

5.3.2. Energy Dispersive X-Ray Spectrometry (EDS) analysis of AG coating

AG coatings determine a decrement of specular reflection by diffusing the light in all the solid angle. This is obtained by means of nano-structured surfaces and the presence of organic or inorganic particles dispersed in the bulk resin. EDS was used to identify the composition of the inorganic particles dispersed in the bulk resin. Moreover, the technique has allowed correlating the results obtained with the presence of the dispersed particles. In fact, EDS spectra were collected, and EDS maps were extracted for all the founded elements to correlate the presence of the element with the dispersed particles. In all the EDS spectra, a peak relative to the presence of Silver (Ag) is present, due to the metallization of the specimen for the analysis.

5.4. Morphological assessment of the materials

The morphological assessment of the materials was performed with Leica DCM 8 optical confocal profilometer. The objectives used are EPI 20x and EPI 50x. The 20x objective was used to analyse all the samples apart from sample 7. For this last sample, the 50x objective was used. The area of investigation is 877x660 μm^2 with the 20x objective and 351x264 μm^2 with the 50x objective. The choice to change the objective for sample 7 is related to the characteristics of the surface. In fact, the surface of this sample is smooth referred to the other samples and the measurements obtained with the objective 20x were not correct at all. On the other hand, the use of the 50x objective for the other samples was not feasible because of the necessity to collect a larger area and to guarantee the collection of all the structures characterising the samples. In Figure 28, the morphological maps collected with the same magnification (50x) of sample 1 and 7 is reported for comparison purpose only.

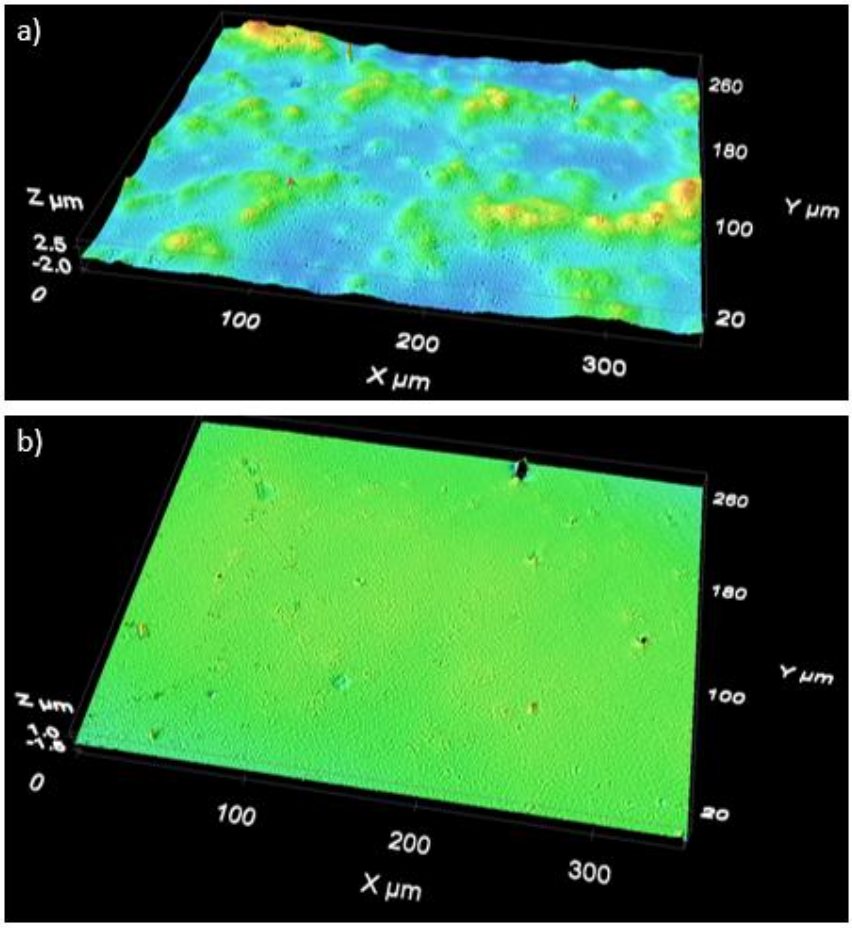

Figure 28: Comparison of acquired maps with 50x objective: a) sample 1; b) sample 7

Starting from the collected morphological maps, different parameters (as defined in paragraph 2.6 and paragraph 4.3.2) were calculated:

- S_a, arithmetical mean deviation of the assessed topographic surface
- S_q, root mean square deviation of the assessed topographic surface
- S_{al}, autocorrelation length
- S_{tr}, texture aspect ratio.

Table 7: Height parameters S_a and S_q of samples under investigation

Sample	Gloss Unit	Elements of particles	S_a (µm)	S_q (µm)	S_{al} (µm)	S_{tr}
1	18.6 ± 0.4	Si, O	1.51 ± 0.07	1.91 ± 0.11	4.4 ± 0.3	0.861 ± 0.014
2	21.9 ± 0.2	Si	1.38 ± 0.15	1.65 ± 0.18	2.54 ± 0.03	0.811 ± 0.003
3	33.3 ± 0.7	Si, O, Al	1.3 ± 0.06	1.63 ± 0.09	3.4 ± 0.2	0.842 ± 0.018
4	40.0 ± 1.1	No inorganic particles	0.84 ± 0.02	1.12 ± 0.02	41 ± 4	0.84 ± 0.08
5	68.5 ± 1.9	Si, O, Al	0.70 ± 0.06	1.04 ± 0.06	3.06 ± 0.03	0.825 ± 0.002
6	75 ± 2	Si, O, Al	0.50 ± 0.02	0.83 ± 0.03	3.0 ± 0.2	0.845 ± 0.05
7	85.7 ± 0.9	No inorganic particles	0.025 ± 0.002	0.035 ± 0.006	25 ± 5	0.61 ± 0.18

The values of the height parameters S_a and S_q, with the relative uncertainty calculated as the standard deviation of three measurements are reported in Table 7. As expected from the literature [38], the values of S_a and S_q are linearly correlated to the gloss values. Figure 29 reports the correlation between gloss and S_a. The coefficient of determination R^2 is equal to 0.93. In Figure 30, instead, the correlation between gloss and S_q is reported. In this case, the coefficient R^2 is equal to 0.86.

Considering the general equation:

$$y = a * x + b$$

(5. 1)

The result of the linear fit between gloss and S_a data is:

- $a_1 = (-48 \pm 16)\ \mu m^{-1}$

- $b_1 = (92 \pm 17)$

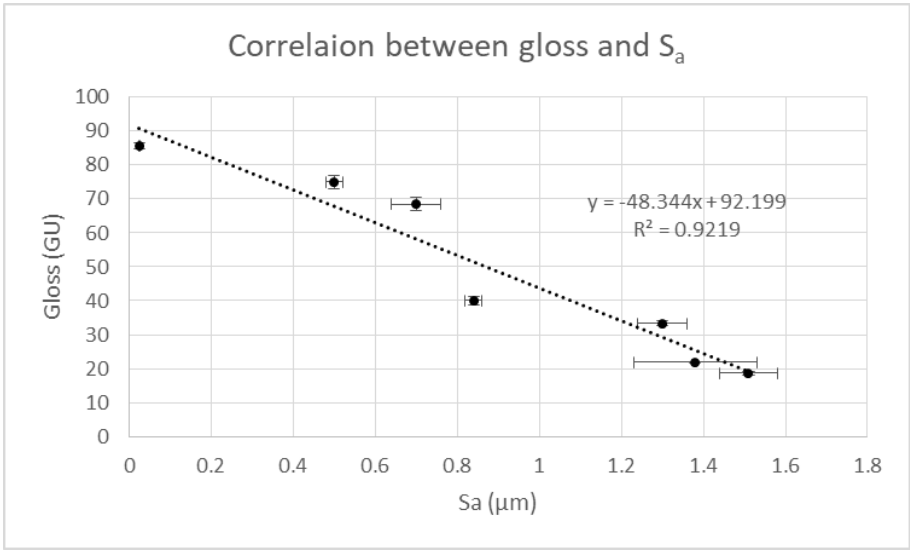

Figure 29: Correlation between Gloss Unit and S_a

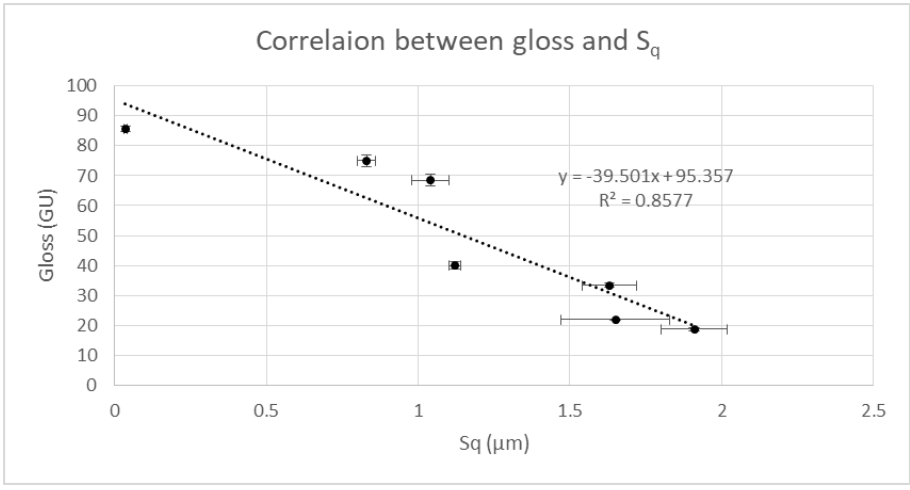

Figure 30: Correlation between Gloss Unit and S_q

Considering the equation (5. 1), the result of the linear fit between gloss and S_q data is:

- $a_2 = (-40 \pm 18)\ \mu m^{-1}$
- $b_2 = (95 \pm 24)$.

The values of the texture aspect ratio, S_{tr}, give a measure of the spatial isotropy or directionality of the surface texture. The results obtained are close to 1 for all the solutions, apart from sample 7; for this reason, all the sample can be considered spatially isotropic textured. Sample 7 shows the lower value of S_{tr}; this is due to small defects of the surface (see Figure 28b). Instead, the presence of defects, which are not isotropically distributed, determines a high value of the autocorrelation length, S_{al}. This value is high also for sample 4 respect to the other samples. As illustrated in Figure 31, the morphology of sample 4 shows structure with dimensions and density of structure higher than the other samples. For this reason, the isotropy analysis on sample 4 were performed with the objective 10x (see Figure 32) that guarantee to collect a higher area (1754 x 1320 μm^2). The values obtained with the objective 10x for sample 4 are reported in Table 8.

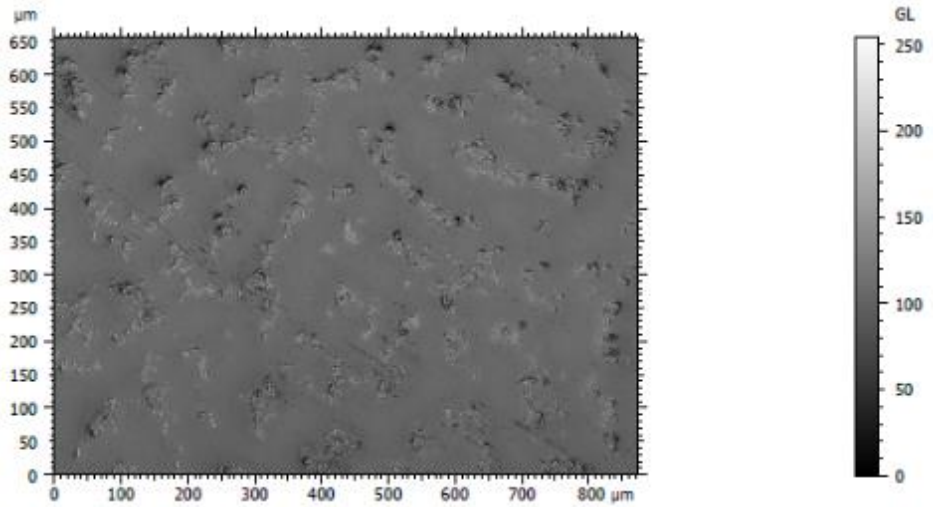

Figure 31: Morphological map in grey scale level of sample 4 with 20x objective

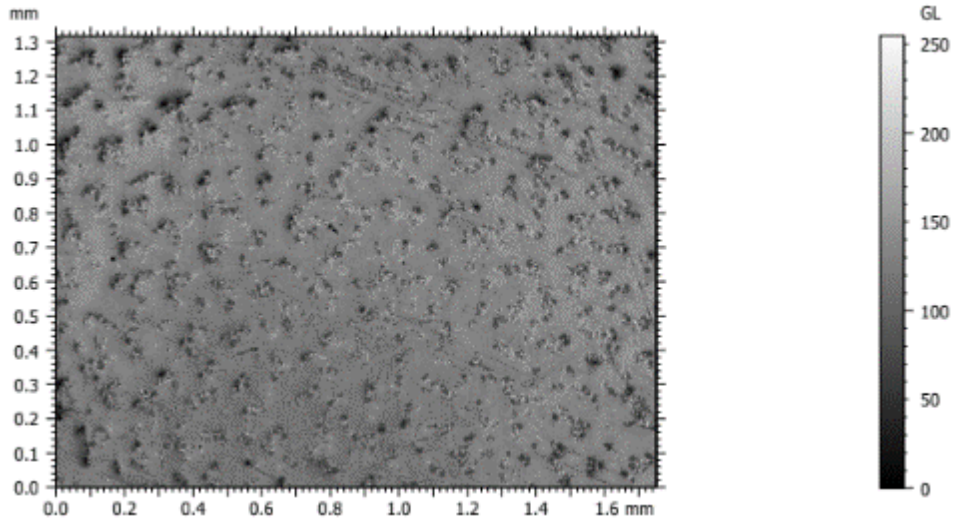

Figure 32: Morphological map in grey scale level of sample 4 with 10x objective

Table 8: Spatial parameters S_{al} and S_{tr} of samples under investigation

Sample	Gloss Unit	Elements of particles	S_{al} (µm)	S_{tr}
1	18.6 ± 0.4	Si, O	4.4 ± 0.3	0.861 ± 0.014
2	21.9 ± 0.2	Si	2.54 ± 0.03	0.811 ± 0.003
3	33.3 ± 0.7	Si, O, Al	3.4 ± 0.2	0.842 ± 0.018
4	40.0 ± 1.1	No inorganic particles	10.3 ± 0.2	0.86 ± 0.05
5	68.5 ± 1.9	Si, O, Al	3.06 ± 0.03	0.825 ± 0.002
6	75 ± 2	Si, O, Al	3.0 ± 0.2	0.845 ± 0.05
7	85.7 ± 0.9	No inorganic particles	25 ± 5	0.61 ± 0.18

5.5. Optical assessment of cover lenses with AG coatings: sparkle effect

In this section, the sparkle effect generated from the different samples is evaluated. For the analysis, the method extracted from FCA standard 7.M0015 [47] (described in paragraph 4.2) is considered.

For the different samples, the results are reported in Table 9. The uncertainty on the S values is calculated as the standard deviation of 10 measurements.

Sample 7 has the lower value of S. This is due to the absence of the AG coating. Moreover, sample 2 and sample 6 are the samples with the AG treatment that show the lower generation of sparkle effect. Sample 1 and sample 4, instead, have the higher values of S. Figure 33 shows the difference between the application of sample 4 and sample 7 on the LCD screen in false colours of luminance scale.

Table 9: Sparkle effect generated from the samples under investigation on LCD

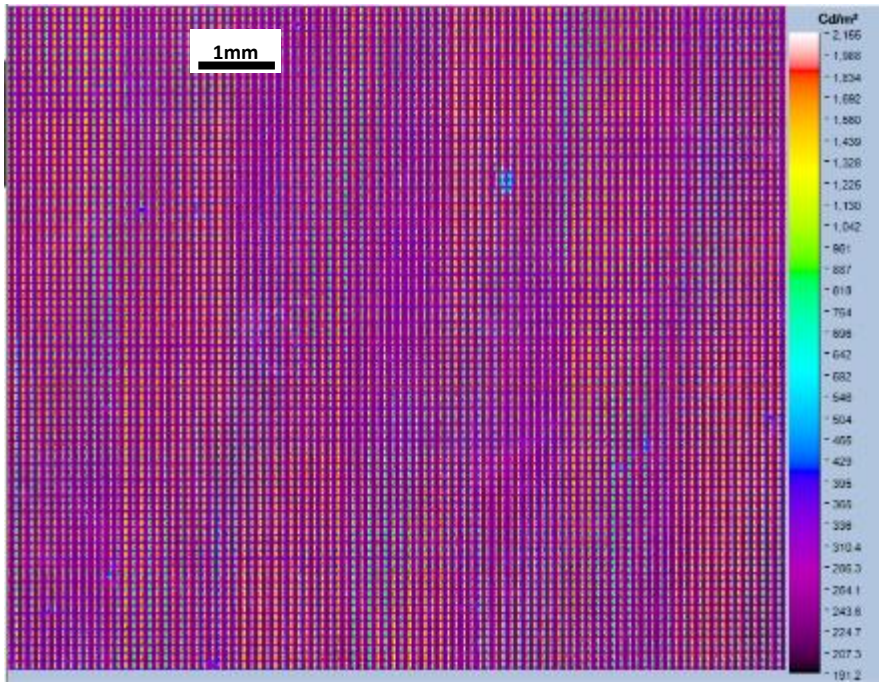

a)

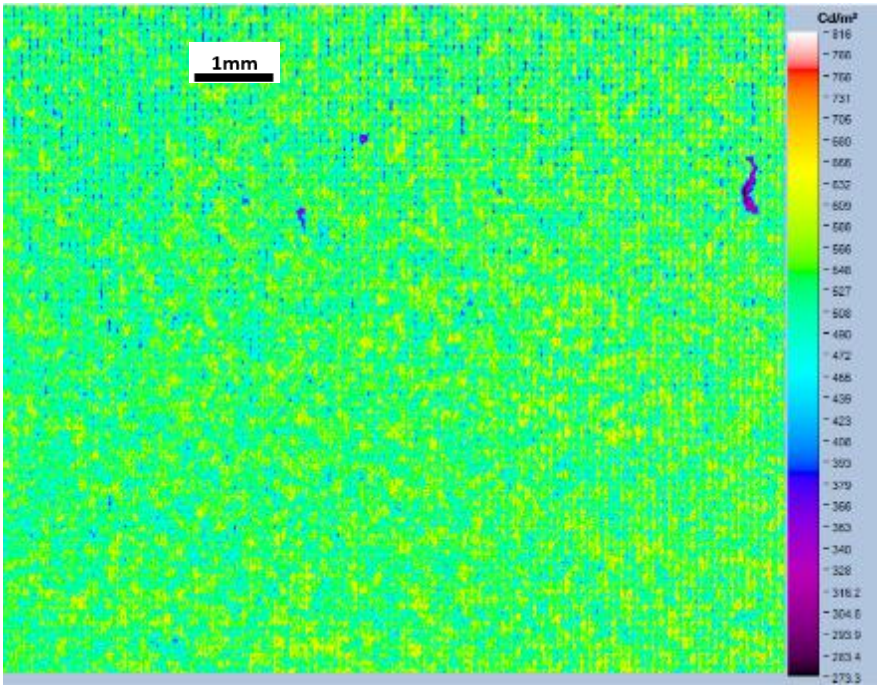

b)

Figure 33: Sample 7 (a image) and sample 4 (b image) on the LCD screen in false colours of luminance scale

In analogy to the work conducted from Huckaby and Cairns [57], the sparkle effect was linearly correlated to the gloss value of the samples under investigation. For the following analyses, sample 7, which has not the AG coating is not considered. It does not exist a linear correlation between sparkle effect, S, and gloss.

5.5.1. Use of polarisation to assess sparkle effect

During the PhD activity, an innovative methodology was developed to assess the sparkle effect due to the optical properties of the anti-glare coatings and the interaction with the light source, e.g., LCD display [54]. The quantification of sparkle effect is performed by analysing the images collected with the developed methodology.

5.6. Conclusions

The samples under testing have been optically characterized in terms of luminous transmittance, reflectance, and haze. The materials composition investigation was

a necessary step to relate the different properties of the solutions under analysis to the materials involved. All the samples are characterised by the presence of acrylic materials in the matrix of AG coating. The AG treatment is obtained by means of inorganic particles for all the samples, except for one sample, for which the analyses have not detect the presence of inorganic particle.

6. Conclusions

6.1. Main conclusions

This work discusses the main future challenges in automotive materials for **display coverlens**. The principal characteristics of an automotive display, its structure and the materials used for the manufacturing of the different parts of the component were described. An overview of the coating deposition techniques and the mains techniques for the manufacturing of display cover lenses was also provided. A particular attention was devoted to the description of AG coatings, the principal material used on top of display cover lenses. The description of this coating includes the principal optical characteristics and the correlation between gloss and haze with the height parameters extracted from morphological analysis.

In literature, there are not well-defined standards for the whole assessment of an automotive display cover lens. For this reason, all the main methodologies for the optical properties evaluation of cover lens were collected and explained. The final goal was to express good display cover lenses metrology in an unambiguous manner and to clearly present measurement methods in a self-contained way.

It was provided a description of:

- methodologies for **aesthetical and surface finishing of materials**, i.e., gloss unit evaluation and haze quantification
- methodologies for the assessment of the morphology of display cover lens
- techniques used for the quantification of **display** optical output variation due to the **interaction with the materials** used for the display cover lenses.

A particular attention was devoted to the assessment and quantification of sparkle effect. An overview of the current methodologies for the assessment of this effect was proposed and the main issues in the application of these methodologies were described. The issues are related to the impossibility to distinguish between sparkle and Moiré effect, the difficulty to properly align the camera detector and the device under testing, the impossibility to eliminate the contribution of the luminance modulation of the display pixels and the impossibility to characterize independently the contribution of the cover lens. Moreover, due to the necessity of a fine alignment, all these techniques are not easily applicable for analysis directly on the

vehicle. All these aspects have made necessary the development of a new system for the quantification of sparkle effect. The new methodology is characterized by using polarized light and allows identifying the area of the surface of the cover lens that generates the sparkle effect. The images collected with this technique were analysed and correlated to the sparkle effect.

The samples under testing have been optically characterized in terms of luminous transmittance, reflectance, and haze. The materials composition investigation was a necessary step to relate the different properties of the solutions under analysis to the materials involved. All the samples are characterised by the presence of acrylic materials in the matrix of AG coating. The AG treatment is obtained by means of inorganic particles for all the samples, except for one sample, for which the analyses have not detected the presence of inorganic particle.

6.2. Future development

The limited number of samples has not allowed deeper investigations on the relationship between the autocorrelation length extracted from the methodology proposed in this thesis and the sparkle effect. The investigation of this relationship will continue after the conclusion of the PhD activity, with the analysis of further commercial samples.

Moreover, the application of the developed methodology and all the other main methodologies for the optical properties' evaluation could be extended and adapted for the assessment of other typologies of devices. An important example is the assessment of materials for automotive ambient lighting. In fact, in this case is also important to deeply investigate how the interaction between the materials and the light sources changes the optical output of the device.

7. Bibliography

1. https://www.databridgemarketresearch.com/reports/global-automotive-display-market
2. https://www.motorionline.com/foto/big/fiat-punto-150/3
3. https://www.techeblog.com/2021-mercedes-s-class-interior/
4. https://www.alvolante.it/primo_contatto/fiat-nuova-500-elettrica
5. https://www.globenewswire.com/news-release/2019/03/27/1773726/0/en/Automotive-Display-Market-to-surpass-30bn-by-2025-Global-Market-Insights-Inc.html
6. https://www.mercedes-benz.it/passenger/cars/the-brandnews-and-eventsnewsmercedes-benz-vision-eqsmercedes-benz-vision-eqs-stage.module.html
7. https://www.mordorintelligence.com/industry-reports/global-automotive-display-market
8. D. Kyriacos, "Polycarbonates", *Brydson's Plastics Materials*, **2017**, Pages 457-485
9. Altuglas International, "Plexiglas UF-3 UF-4 and UF-5 sheets", Wayback Machine. Plexiglas.com, **2012**
10. M.F. Ashby, D. Cebon, "Materials selection in mechanical design", *Le Journal de Physique IV*, *3*(C7), C7-1, **1993**
11. https://www.saint-gobain-sekurit.com/global-excellence/our-production-processes/glossary
12. G.P. Kothiyal, G.K. Dey, "Glass and Glass-Ceramics", *Functional Materials*, **2012**
13. Bent Glass Design, "A Brief Explanation of Chemically Strengthened Glass", *www.bentglassdesign.com*, **2016**
14. N. Li Pira, "Handbook of Flexible Organic Electronics", *Woodhead Publishing, Chapter 14, 346-374*, **2015**
15. https://v1industrial.com/in-mold-decoration-labeling.html
16. http://www.canon-slade.bolton.sch.uk/microsites/Tech/knowledge%20folder/Y11_GR_manu_cal.html
17. https://polymeracademy.com/plastic-processing-techniques/
18. A. Trajkovska-Petkoska, I. Nasov, "Surface engineering of polymers: Case study: PVD coatings on polymers.", *Zaštita materijala, 55(1), 3-10*, **2014**

19. P.M. Martin, “Handbook of Deposition Technologies for Films and Coatings”, *Elsevier,* III-rd Ed, **2000**
20. G. Faraji, H. S. Kim, H. T. Kashi, “Sever Plastic Deformation”, *Elsevier, 1-17*, **2018**
21. M. Miller, “Slot die coating technology”, *Coating Tech*, **2014**
22. J. Park, K. Shin, C. Lee, "Roll-to-Roll Coating Technology and Its Applications: A Review". International Journal of Precision Engineering and Manufacturing.,17 (4): 537–550, **2016**
23. FOM Technologies, "Slot die coating technology”, **2020**
24. R. Patidar, D. Burkitt, K. Hooper, D. Richards, T. Watson, “Slot-die coating of perovskite solar cells: An overview”, *Materials Today Communications, Vol. 22*, **2020**
25. J. Bosmans, “Flow Coating combines high performance with top quality results”, *Sirris*, **2018**.
26. D. M. Barber, A. J. Crosby, T. Emrick, “Mesoscale Block Copolymers”, *Advanced Materials*, **2018**
27. F. Scaffidi Muta, R. Daanyal, N. Li Pira, “COATINGS PERFORMANCE REQUIREMENTS FOR DISPLAY COVER LENSES”, *FCA standard MS.90165*, **2021**
28. M. Ulzio, “OPTICAL PROPERTIES OF GLASS: HOW LIGHT AND GLASS INTERACT”, *Koop Glass*, **2015**
29. W. H. Southwell, “Gradient-index antireflection coatings”, *Opt. Lett*. 8 (11), 584 **1983**
30. C. Chang, C. Chen, F. Hwang, C. Chen and L. Cheng, “Preparation of polymer/silica composite antiglare coatings on poly(ethylene terephathalate) (PET) substrates”, *Coat. Technol. Res*., 9 (5) 561–568, **2012**
31. https://www.andersdx.com/anti-glare-vs-anti-reflective-what-is-the-difference/
32. Y. Huang, L. Chen, H. Chou, “Optimization of Process Parameters for Anti-Glare Spray Coating by Pressure-Feed Type Automatic Air Spray Gun Using Response Surface Methodology”, *MDPI Materials,* **2019**
33. C. H. Min, Y. S. Kang, T. S. Kim, “Modeling and Recipe Optimization of Anti-Glare Process Using Sandblasting for Electronic Display Glass”, *MDPI Electronics*, **2020**
34. N. Nguyen, “Fabrication technologies”, *Micromixers, II Edition*, **2012**

35. A. J. Sanchez-Herencia, "Water Based Colloidal Processing of Ceramic Laminates", *Trans Tech Publications*, **2007**
36. K. Vessot, P. Messier, J. M. Hyde, C. A. Brown, "Correlation between gloss reflectance and surface texture in photographic paper", *Scanning, 37(3), 204-217*, **2015**
37. N. J. Elton, J. C. C. Day, "A reflectometer for the combined measurement of refractive index, microroughness, macroroughness and gloss of low-extinction surfaces", *Measurement Science and Technology, 20(2),* **2009**
38. Q. Yong, J. Chang, Q. Liu, F. Jiang, D. Wei, H. Li, "Matt Polyurethane Coating: Correlation of Surface Roughness on Measurement Length and Gloss", *Polymers, 12(2), 326*, **2020**
39. ASTM D1003-07, "Standard Test Method for Haze and Luminous Transmittance of Transparent Plastics", *ASTM International*, **2007**
40. E. Andreassen, Å. Larsen, K. Nord-Varhaug, M. Skar, H. Øysæd, "Haze of polyethylene films—effects of material parameters and clarifying agents", *Polymer Engineering & Science, 42(5), 1082-1097*, **2002**
41. ISO 25178-2:2012, "Geometrical product specifications (GPS) — Surface texture: Areal — Part 2: Terms, definitions and surface texture parameters", **2012**
42. M. Juuti, & al, "Detection of local specular gloss and surface roughness from black prints. Colloids Surf. A", *Physicochem. Eng. Asp., 299, 101–108*, **2007**
43. https://www.ophiropt.com/laser--measurement/knowledge-center/article/10145
44. D. Soliman, "Augmented microscopy: Development and application of high-resolution optoacoustic and multimodal imaging techniques for label-free biological observation", *Ph.D. Thesis*, **2016**
45. R. Beaty, "Current display testing", *Radiant Vision Systems*, **2017**
46. A. Ryer, "Light measurement handbook", *International Light*, **1998**
47. L. Belforte, N. Li Pira, "METHOD FOR THE OPTICAL CHARACTERIZATION OF AN AUTOMOTIVE DISPLAY", *FCA standard 7.M0015*, **2017**
48. "Information Display measurements Standard", *International Committee for Display Metrology,* **2012**.
49. M.E. Becker, J. Neumeier, "Optical Characterization of Scattering Anti-Glare-Layers", *SID Symposium Digest of Technical Papers*, **2011**

50. D. R. Cairns and P. Evans, "Laser speckle of textured surfaces: towards high performance anti-glare surfaces," *SID Symposium Digest of Technical Papers 38, No. 1, 407–409*, **2007**.
51. J. Gollier, G. A. Piech, S. D. Hart, J. A. West, H. Hovagimian, E. M. Kosik Williams, A. Stillwell, J. Ferwerda, "Display Sparkle Measurement and Human Response", *Journal of SID (44:1), 295-297,* **2013**
52. D. N. Sidrov and A. C. Kokaram, "Suppression of moiré patterns via spectral analysis", *Proceedings of SPIE (4671), 895-906*, **2002**
53. https://stringfixer.com/tags/moir%C3%A9
54. F. Scaffidi Muta, L. Belforte, N. Li Pira, "Device for detecting the sparkle effect of a transparent sample", *EU -EP3719565A1 - US2020310171A1*, **2021**
55. https://www.keyence.com/ss/products/microscope/roughness/surface/sal-auto-correlation-length.jsp
56. https://physics.nist.gov/PhysRefData/Star/Text/ESTAR.html
57. D. K. P. Huckaby and D. R. Cairns, "Quantifying sparkle of anti-glare surfaces," *SID Symposium of Technical Papers 40, No. 1, 511–513*, **2009**
58. MountainsMaps, "Surface Imaging and Metrology software", *DigitalSurf,* **2006**

Acknowledgment

The present work could not be possible without the support of several people.

First, I would like to thank all my colleagues at Centro Ricerche FIAT, in Materials & Sustainability Engineering for the support, knowledge, expertise and experience. A special thanks to Dr. Li Pira that supported me in my daily research activity, driving me and discussing with me the several issues met during the experimental activity. Moreover, He also gave me the chance to take part to seminars and lectures and gave me the opportunity to collaborate with the University of Thessaloniki and OET company for the development of my thesis abroad. Here I met experienced researchers and wonderful friends; I will always be grateful to them.

I am also grateful to Solid State Physics Group at Physics Department of the University of Turin. A particular thanks to Dr. Picollo that supported me during the research period from technical point of view to more bureaucratic aspects.

Last, thanks to my love Alessia, my parents, my Family and my Friends, for their presence and support along this period.

Annex A

Optical assessment of the aesthetical and surface finishing of the materials: experimental methods

The **aesthetical and surface finishing** of the materials used for display cover lenses is evaluated with different optical techniques. The main Min methodologies used in this work are described:

5. **Gloss Unit** (GU) detection
6. **Haze** evaluation
7. **Luminous transmittance and reflectance** of the materials
8. **Morphological** analysis

Gloss (see paragraph 2.6 for the definition) has been extensively used in the coating industry to describe the reflectance properties of a coating. It is one of the most important indicators used to describe the visual effect of an object [36].
In this work, a Rhopoint Dualgloss IQ meter was used on **black samples** to confirm the gloss values reported in the datasheets of commercial samples that have been analysed.

Figure 34: Rhopoint Dual gloss IQ gloss meter

The **optical finishing of transparent samples** was analysed by means of ***Haze*** measurements according to ASTM D1003-07 [39].

Figure 35: Konica Minolta CM3610A spectrophotometer

As described in the next paragraphs, Konica Minolta CM3610-A spectrophotometer was used to measure the level of haze. The CM-3610A Spectrophotometer is a high precision, high-reliability bench-top instrument with vertical alignment that can measure in reflectance or in transmittance mode. The detector is a silicon photodiode array; the spectral dispersive device is a diffraction grating and the wavelength range is 360 to 780 nm.

The ***luminous transmittance and reflectance*** of the materials was investigated with Varian Cary 500 spectrophotometer. The spectrophotometric analysis consists in illuminating the sample with light at a specific wavelength and detecting the amount of reflected or transmitted light. Usually, spectrophotometers work in the UV and visible (VIS) regions of the electromagnetic spectrum, but there are some instruments that operate also in the infrared (IR) region. The principal difference is the type of detector used. Moreover, the measurements in the IR regions can be affected, for wavelength higher than 5µm, by thermal emission of the samples.

The Varian Cary 500 spectrophotometer, used in this work (Figure 36), allows investigating a range of wavelength starting from 175nm up to 3300nm. This range

is obtained by means of two lamps: a deuterium lamp for the UV emission (175 – 300nm) and a halogen lamp for the VIS/IR (300 – 3300nm). The instrument has a high spectral resolution obtained by a system of two monochromators with double grating. The Cary 500 has two detectors: a photomultiplier to detect in the UV/VIS region and a lead sulphide (PbS) sensor to detect the IR emission.

This spectrophotometer works using a double beam: a chopper is used to deviate the light radiation alternatively sent to the sample under investigation or to a reference material. This alternation allows the spectrophotometer measuring the absolute transmittance and reflectance values, avoiding errors due to the instability of the light sources.

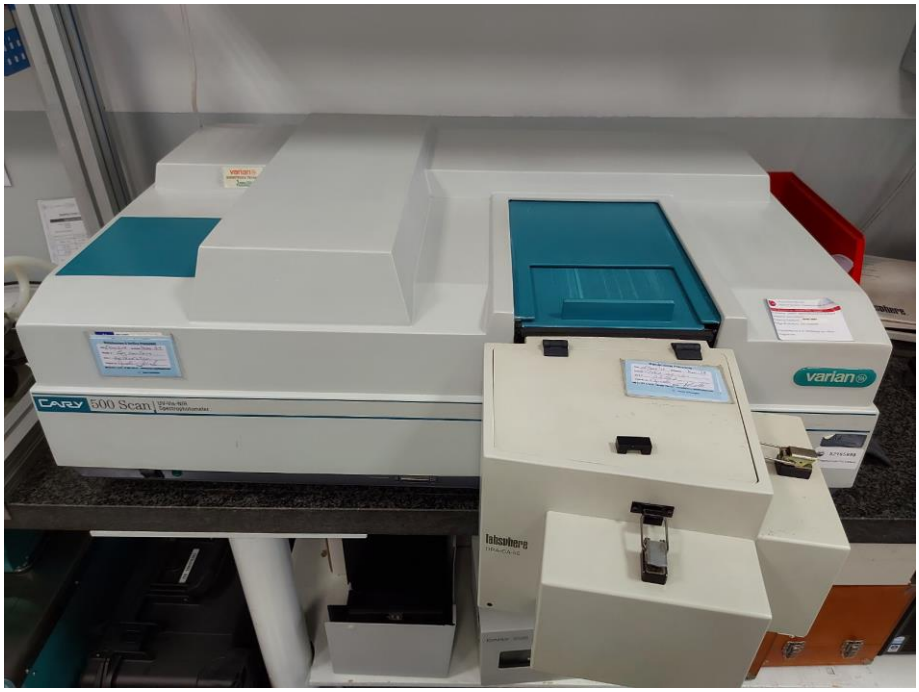

Figure 36: Varian Cary 500

The instrument can be assembled with different tools for the assessment of specular reflectance at different angles of incidence of the light (Varian Cary VASRA) or with an integrating sphere (Labsphere) for the evaluation of total transmittance (direct and diffused transmitted light), total reflectance (specular and diffused reflected light) and diffused reflected light. Figure 37 shows the functional scheme of the

integrating sphere: a hollow sphere with internal walls of Spectralon, a fluoropolymer that has the highest light diffusivity in the UV, VIS and IR regions of electromagnetic spectrum than any other materials or coating known. The reflectance measurements are done by placing the sample on a second port in the integrating sphere, opposite to the input port. In Varian spectrophotometer, the light incident angle is set to 8°. The measurements of only diffused reflected light are performed by placing a black light trap in the portion of the integrating sphere correspondent to the specular reflectance direction. In this way, the contribution of the specular reflection is eliminated. The total transmittance measurements are performed by placing the sample on the input port. The light trap in not applied and in correspondence of the second port, a Spectralon sample is applied.

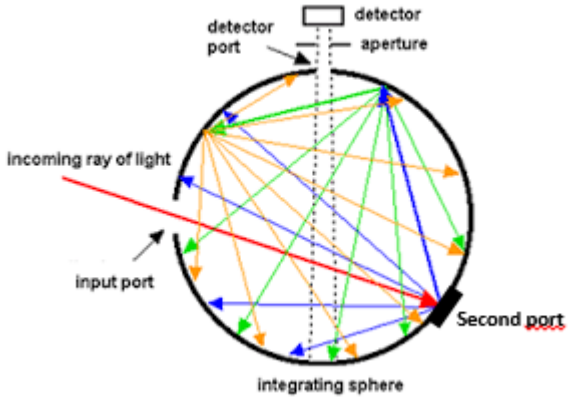

Figure 37: Functional scheme of integrating sphere [43]

The ***morphological*** analysis of the samples was performed with an optical confocal microscope. This instrument allows the morphological structures of the surfaces at sub-microns scales to be investigated. The confocal analysis allows the collection of 3D images with high definition, by avoiding the presence of halos due to unfocused areas. Optical confocal microscopes can operate in transmission or in reflection mode. In Figure 38 the functional scheme of optical confocal microscope for analysis in reflection mode is reported. It is characterized by a coherent light source (e.g. LASER) or incoherent light source (e.g. LED). The use of an incoherent light source lets colours imaging but requires the use of expensive lenses and optics for the correction of chromatic aberrations [44]. Moreover, it is necessary the adoption of light collection systems because the light emission is almost isotropic.

The incoherent light as source is particularly used for the observation of samples characterized by periodical geometrical structures. In fact, when these kinds of structures are illuminated by coherent light, a distortion of the image occurs due to the interference of the reflected light by the internal layers of the structure.
The coherent source (i.e. a laser) is particularly suitable for the monochromatic and collimated light emission whit a lower cost. The monochromaticity of the light simplifies the design of lenses and filters, with a consequent reduction of the costs. Moreover, by creating a RGB system by means of different laser sources, the colours imaging became possible.

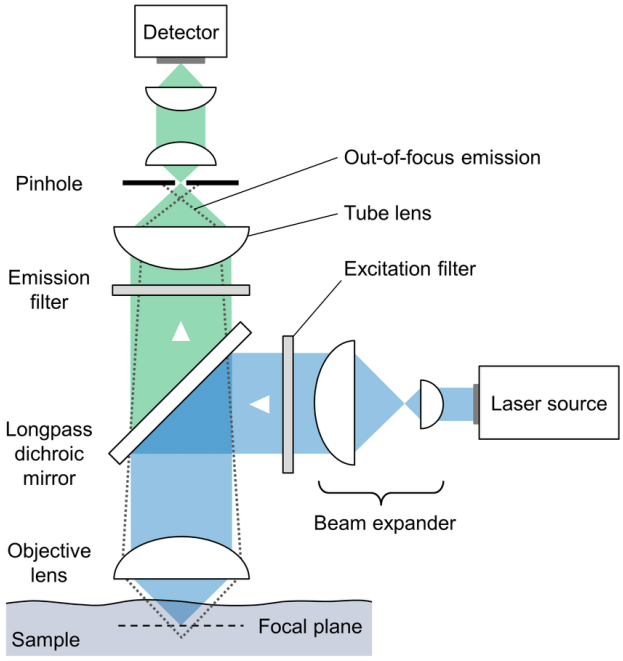

Figure 38: Functional scheme of optical confocal microscope for analysis in reflection mode [44]

The role of the light source is to provide stable and brilliant light in order to collect a useful signal coming from the sample despite the presence of the pinholes. A pinhole is a component characterized by a circular hole. The diameter is in between few micrometres up to hundred micrometres. In the confocal systems, two pinholes are adopted: the illumination pinhole and the detection pinhole. The illumination pinhole allows having a point-like beam. After the first pinhole, a beam splitter is present to split the beam in two parts. Then, the beam is focused on the sample by the objective. By interacting with the sample, the beam is reflected and focalized on

the detection pinhole. In this way, it can be selected the reflected beam from a specific focal plane.

The optical confocal microscope used in this work is a Leica DCM8 (Figure 39). It works in reflection mode and allows the coupling of the confocal and interferometric techniques. The confocal technique offers a high lateral resolution (100s of nanometres); the interferometric techniques is required to have a nanometre resolution axially. The sample is vertically analysed; in this way all the points of the surface are in the focal scan range. The light source is characterized by four LEDs for HD RGB colour imaging. The peak emission of the LEDs is 630nm for the red LED, 530nm for the green and 460nm for the blue. The fourth LED lets have white light emission centred on 550nm. The light intensity is tuneable in order to avoid the saturation of the CCD detector in case of high reflection intensity or vice versa to fail the acquisition due to the low intensity of the reflected light.

Figure 39: Leica DCM8 optical confocal microscope

The selection of the objective for the analysis is driven by the later resolution and the vertical resolution required for the image. As example, a numerical aperture of 0.95* and high magnification allows obtaining a later resolution up to 140nm and a

vertical resolution up to 2nm. The objectives available at Centro Ricerche FIAT labs are:

- EPI 10x
- EPI 20x
- EPI 50x
- EPI 150x

The main characteristics of the objectives are herein reported:

Confocal Mode

Objective Magnification	1.25×	2.5×	5×	10×	20×	50×	100×	150×
Numerical Aperture	0.04	0.07	0.15	0.3	0.5	0.9	0.95	0.95
Field of View (FOV) (µm)	14032 x 10560	7016 x 5280	3508 x 2640	1754 x 1320	877 x 660	351 x 264	175 x 132	117 x 88
Optical Resolution (x/y (µm)	3.5	2.0	0.94	0.47	0.28	0.16	0.14	0.14
Vertical Resolution (nm)	<3000	<350	<150	<30	<15	<5	<2	<2
Typical Measurement Time	3 – 5 seconds							

Annex B

Samples description